IEC TR 60747-5-12

Edition 1.0 2021-10

TECHNICAL REPORT

Semiconductor devices –
Part 5-12: Optoelectronic devices – Light emitting diodes – Test method of LED efficiencies

IEC TR 60747-5-12:2021-10(en)

IEC Central Office
3, rue de Varembé
CH-1211 Geneva 20
Switzerland

Tel.: +41 22 919 02 11
info@iec.ch
www.iec.ch

About the IEC
The International Electrotechnical Commission (IEC) is the leading global organization that prepares and publishes International Standards for all electrical, electronic and related technologies.

About IEC publications
The technical content of IEC publications is kept under constant review by the IEC. Please make sure that you have the latest edition, a corrigendum or an amendment might have been published.

IEC publications search - webstore.iec.ch/advsearchform
The advanced search enables to find IEC publications by a variety of criteria (reference number, text, technical committee, …). It also gives information on projects, replaced and withdrawn publications.

IEC Just Published - webstore.iec.ch/justpublished
Stay up to date on all new IEC publications. Just Published details all new publications released. Available online and once a month by email.

IEC Customer Service Centre - webstore.iec.ch/csc
If you wish to give us your feedback on this publication or need further assistance, please contact the Customer Service Centre: sales@iec.ch.

IEC online collection - oc.iec.ch
Discover our powerful search engine and read freely all the publications previews. With a subscription you will always have access to up to date content tailored to your needs.

Electropedia - www.electropedia.org
The world's leading online dictionary on electrotechnology, containing more than 22 000 terminological entries in English and French, with equivalent terms in 18 additional languages. Also known as the International Electrotechnical Vocabulary (IEV) online.

IEC TR 60747-5-12

Edition 1.0 2021-10

TECHNICAL REPORT

colour inside

Semiconductor devices – Part 5-12: Optoelectronic devices – Light emitting diodes – Test method of LED efficiencies

INTERNATIONAL ELECTROTECHNICAL COMMISSION

ICS 31.080.99

ISBN 978-2-8322-1035-9

CONTENTS

INTERNATIONAL ELECTROTECHNICAL COMMISSION

_____

SEMICONDUCTOR DEVICES –

Part 5-12: Optoelectronic devices – Light emitting diodes – Test method of LED efficiencies

FOREWORD

1) The International Electrotechnical Commission (IEC) is a worldwide organization for standardization comprising all national electrotechnical committees (IEC National Committees). The object of IEC is to promote international co-operation on all questions concerning standardization in the electrical and electronic fields. To this end and in addition to other activities, IEC publishes International Standards, Technical Specifications, Technical Reports, Publicly Available Specifications (PAS) and Guides (hereafter referred to as "IEC Publication(s)"). Their preparation is entrusted to technical committees; any IEC National Committee interested in the subject dealt with may participate in this preparatory work. International, governmental and non-governmental organizations liaising with the IEC also participate in this preparation. IEC collaborates closely with the International Organization for Standardization (ISO) in accordance with conditions determined by agreement between the two organizations.
2) The formal decisions or agreements of IEC on technical matters express, as nearly as possible, an international consensus of opinion on the relevant subjects since each technical committee has representation from all interested IEC National Committees.
3) IEC Publications have the form of recommendations for international use and are accepted by IEC National Committees in that sense. While all reasonable efforts are made to ensure that the technical content of IEC Publications is accurate, IEC cannot be held responsible for the way in which they are used or for any misinterpretation by any end user.
4) In order to promote international uniformity, IEC National Committees undertake to apply IEC Publications transparently to the maximum extent possible in their national and regional publications. Any divergence between any IEC Publication and the corresponding national or regional publication shall be clearly indicated in the latter.
5) IEC itself does not provide any attestation of conformity. Independent certification bodies provide conformity assessment services and, in some areas, access to IEC marks of conformity. IEC is not responsible for any services carried out by independent certification bodies.
6) All users should ensure that they have the latest edition of this publication.
7) No liability shall attach to IEC or its directors, employees, servants or agents including individual experts and members of its technical committees and IEC National Committees for any personal injury, property damage or other damage of any nature whatsoever, whether direct or indirect, or for costs (including legal fees) and expenses arising out of the publication, use of, or reliance upon, this IEC Publication or any other IEC Publications.
8) Attention is drawn to the Normative references cited in this publication. Use of the referenced publications is indispensable for the correct application of this publication.
9) Attention is drawn to the possibility that some of the elements of this IEC Publication may be the subject of patent rights. IEC shall not be held responsible for identifying any or all such patent rights.

IEC TR 60747-5-12 has been prepared by subcommittee 47E: Discrete semiconductor devices, of IEC technical committee 47: Semiconductor devices. It is a Technical Report.

The text of this Technical Report is based on the following documents:

Draft	Report on voting
47E/741/DTR	47E/748/RVDTR

Full information on the voting for its approval can be found in the report on voting indicated in the above table.

The language used for the development of this Technical Report is English.

This document was drafted in accordance with ISO/IEC Directives, Part 2, and developed in accordance with ISO/IEC Directives, Part 1 and ISO/IEC Directives, IEC Supplement, available at www.iec.ch/members_experts/refdocs. The main document types developed by IEC are described in greater detail at www.iec.ch/standardsdev/publications.

A list of all parts in the IEC 60747 series, published under the general title *Semiconductor devices*, can be found on the IEC website.

The committee has decided that the contents of this document will remain unchanged until the stability date indicated on the IEC website under webstore.iec.ch in the data related to the specific document. At this date, the document will be

- reconfirmed,
- withdrawn,
- replaced by a revised edition, or
- amended.

IMPORTANT – The "colour inside" logo on the cover page of this document indicates that it contains colours which are considered to be useful for the correct understanding of its contents. Users should therefore print this document using a colour printer.

INTRODUCTION

The latest international standards for light emitting diode (LED) devices are IEC 60747-5-6:2016, IEC 60747-5-8:2019, IEC 60747-5-9:2019, IEC 60747-5-10:2019, and IEC 60747-5-11:2019, where terminology and measuring methods of basic electrical and optical characteristics of LEDs are given.

This technical report gives guidance on the terminology and the measuring methods of various efficiencies of single light emitting diode (LED) chip or package without phosphor. White LEDs for lighting applications are out of the scope of this part of IEC 60747-5-12.

The efficiencies whose measuring methods are described in this technical report are the power efficiency (PE), the external quantum efficiency (EQE), the voltage efficiency (VE), the internal quantum efficiency (IQE), and the light extraction efficiency (LEE). To measure these efficiencies separately, one needs the measurement data of the internal quantum efficiency (IQE).

The IQE is a key performance parameter that represents the quality of epitaxial wafers and contains essential information on operational mechanisms. Requirements for accurate and reliable IQE measurements are suggested. The various IQE measurement methods reported so far are reviewed in detail from a theoretical and practical point of view. Subsequently, the technical limitations for these IQE measurement methods to meet the requirements for accurate and reliable IQE measurements are discussed.

In particular, two different measuring methods of the IQE that can meet the requirements are described in detail both experimentally and theoretically. They are known as the temperature-dependent electroluminescence (TDEL) and the room-temperature reference-point method (RTRM).

A measuring procedure of PE, EQE, VE, IQE, and LEE are demonstrated. But the injection efficiency (IE) and the radiative efficiency (RE) are described for definitions only.

Separate knowledge of various efficiencies of the LED chip or package is able to improve optoelectronic performances of LED chip itself and to design LED application systems such as LED lamps more efficiently and reliably.

SEMICONDUCTOR DEVICES –

Part 5-12: Optoelectronic devices – Light emitting diodes – Test method of LED efficiencies

1 Scope

This technical report discusses the terminology and the measuring methods of optoelectronic efficiencies of single light emitting diode (LED) chip or package without phosphor. White LEDs for lighting applications are out of the scope of this part.

This technical report provides guidance on

– terminology of optoelectronic efficiencies of single LED chip or package without phosphor, such as the power efficiency (PE), the external quantum efficiency (EQE), the voltage efficiency (VE), the light extraction efficiency (LEE), the internal quantum efficiency (IQE), the injection efficiency (IE), and the radiative efficiency (RE) [1][1];

– test methods of optoelectronic efficiencies of the PE, the EQE, the VE, the LEE, and the IQE [1];

– review of various IQE measurement methods reported so far in view of accuracy and practical applicability;

– the measuring method of the LED IQE based on the temperature-dependent electroluminescence (TDEL) [2];

– the measuring method of the LED IQE based on the room-temperature reference-point method (RTRM) [3];

– the measuring method of the radiative and nonradiative currents of an LED [4];

– the relationship between the IQE and the VE, which leads to introduction of a new LED efficiency, the active efficiency (AE) as AE = VE × IQE.

2 Normative reference

The following document is referred to in the text in such a way that some or all of their content constitutes requirements of this document. For dated references, only the edition cited applies. For undated references, the latest edition of the referenced document (including any amendments) applies.

IEC 60747-5-6, *Semiconductor devices – Part 5-6: Optoelectronic devices – Light emitting diodes*

3 Terms and definitions

For the purposes of this document, the following terms and definitions apply.

ISO and IEC maintain terminological databases for use in standardization at the following addresses:

- IEC Electropedia: available at http://www.electropedia.org/
- ISO Online browsing platform: available at http://www.iso.org/obp

[1] Numbers in square brackets refer to the Bibliography.

3.1 General terms and definitions

3.1.1
radiant power
Φ_e
change in radiant energy with time

Note 1 to entry: The unit used is: W. Radiant power is also known as "radiant flux".

[SOURCE: IEC 60050-845:2020, 845-21-038, modified – Note 1 has been expanded.]

3.1.2
spectral distribution
density of a radiant power Φ_e, with respect to wavelength, λ, at the wavelength λ

$$\Phi_{e,\lambda} = \frac{d\Phi_e(\lambda)}{d\lambda}$$

[SOURCE: IEC 60050-845:2020, 845-21-029, modified – In the definition, "a radiant or luminous or photon quantity $X(\lambda)$" has been replaced by "a radiant power Φ_e ". In the formula, X has been replaced by Φ_e. Notes have been deleted.]

3.1.3
mean photon energy
$h\bar{\nu}$
mean energy that each photon carries

$$h\bar{\nu} = \frac{\Phi_e}{\int \frac{\lambda}{hc} \Phi_{e,\lambda} d\lambda}$$

where

h is the Planck constant;

c is the speed of light in vacuum

[SOURCE: IEC 60747-5-8:2019, 3.1.3]

3.2 Terms and definitions relating to the optoelectronic efficiencies

3.2.1
power efficiency
η_{PE}
ratio of the radiant power (coupled to free space), Φ_e, to the electrical power consumed by the LED, $V_F I_F$, where V_F is the forward voltage and I_F is the forward current of the LED

$$\eta_{PE} = \frac{\Phi_e}{V_F I_F}$$

Note 1 to entry: Power efficiency is also known as the "wall-plug efficiency". Power efficiency is identical to the "radiant efficiency" when the power dissipated by any auxiliary equipment is excluded from the electrical power.

[SOURCE: IEC 60747-5-8:2019, 3.2.1]

3.2.2
voltage efficiency
η_{VE}
ratio of the mean photon energy emitted from the LED to the electron energy given by the forward voltage of the LED, V_F

$$\eta_{VE} = \frac{h\bar{\nu}}{qV_F}$$

where

q is the elementary charge.

Note 1 to entry: Voltage efficiency can be greater than 1 at very low forward currents.

[SOURCE: IEC 60747-5-8:2019, 3.2.2]

3.2.3
external quantum efficiency
η_{EQE}
ratio of the number of photons emitted into the free space per unit time to the number of electrons injected into the LED per unit time

$$\eta_{EQE} = \frac{\Phi_e / h\bar{\nu}}{I_F / q}$$

[SOURCE: IEC 60747-5-8:2019, 3.2.3]

3.2.4
internal quantum efficiency
η_{IQE}
ratio of the number of photons emitted from the active region per unit time to the number of electrons injected into the LED per unit time

$$\eta_{IQE} = \frac{\Phi_{e,active} / h\bar{\nu}}{I_F / q}$$

where

$\Phi_{e,active}$ is the radiant power emitted from the active region.

[SOURCE: IEC 60747-5-8:2019, 3.2.4]

3.2.5
light extraction efficiency
η_{LEE}
ratio of the number of photons emitted into the free space to the number of photons emitted from the active region

$$\eta_{\mathrm{LEE}} = \frac{\Phi_{\mathrm{e}}}{\Phi_{\mathrm{e,active}}}$$

[SOURCE: IEC 60747-5-8:2019, 3.2.5]

3.2.6
injection efficiency
η_{IE}
ratio of the number of electrons injected into the active region per unit time to the number of electrons injected into the LED per unit time

$$\eta_{\mathrm{IE}} = \frac{I_{\mathrm{F,active}}}{I_{\mathrm{F}}}$$

where

$I_{\mathrm{F,active}}$ is the portion of the forward current injected into the active region.

[SOURCE: IEC 60747-5-8:2019, 3.2.6]

3.2.7
radiative efficiency
η_{RE}
ratio of the number of photons emitted from the active region per unit time to the number of electrons injected into the active region per unit time

$$\eta_{\mathrm{RE}} = \frac{\Phi_{\mathrm{e,active}} / h\bar{\nu}}{I_{\mathrm{F,active}} / q}$$

[SOURCE: IEC 60747-5-8:2019, 3.2.7, modified – The specific use in angle brackets as well as the note have been removed.]

3.3 Terms and definitions relating to measuring the efficiencies

3.3.1
peak EQE point
set of operating conditions of the forward current and radiant power at which the EQE is the maximum for a given temperature.

Note 1 to entry: The forward current and radiant power at the peak EQE point are denoted as I_{peak} and Φ_{peak}, respectively.

[SOURCE: IEC 60747-5-9:2019, 3.1.6]

3.3.2
cryogenic temperature
temperature range below 200 K

[SOURCE: IEC 60747-5-9:2019, 3.1.7]

3.3.3
critical cryogenic temperature
T_c
cryogenic temperature at which the peak EQE shows the maximum value

[SOURCE: IEC 60747-5-9:2019, 3.1.9]

3.3.4
normalized variables of X and Y
converted quantities of current and radiant power as follows:

$$X = \sqrt{\Phi_e(I_F) / \Phi_e(I_{peak})}$$

$$Y = I_F / I_{peak}$$

[SOURCE: IEC 60747-5-10:2019, 3.1.7]

3.3.5
coefficients of a_1 and a_2
coefficients of the quadratic equation of Y in X, i.e., $Y = a_1 X + a_2 X^2$
Note 1 to entry: a_1 and a_2 change slowly enough according to the forward current as compared to X and Y, but should be treated as a function of the forward current in the data analysis.

[SOURCE: IEC 60747-5-10:2019, 3.1.8]

3.3.6
reference point
operating point at which a_2 is minimum

Note 1 to entry: a_2, X, and Y at the reference point are represented by $a_{2,ref}$, X_{ref}, and Y_{ref}, respectively. The current at the reference point is denoted as $I_{F,ref}$.

[SOURCE: IEC 60747-5-10:2019, 3.1.9]

3.4 Terms and definitions relating to measuring current components

3.4.1
radiative current
I_{rad}
current that is consumed by the radiative recombination process in the LED

[SOURCE: IEC 60747-5-11:2019, 3.1.2]

3.4.2
nonradiative current
I_{nonrad}
current that is consumed by the nonradiative recombination processes in the LED

[SOURCE: IEC 60747-5-11:2019, 3.1.3, modified – The notes have been removed.]

3.5 Abbreviated terms

AE active efficiency
CW continuous wave
EL electroluminescence

EQE	external quantum efficiency
IDPL	intensity-dependent photoluminescence
IE	injection efficiency
IQE	internal quantum efficiency
LED	light emitting diode
LEE	light extraction efficiency
MQW	multiple quantum well
PE	power efficiency
PL	photoluminescence
QW	quantum well
RE	radiative efficiency
RTRM	room-temperature reference-point method
SRH	Shockley-Read-Hall
TDEL	temperature-dependent electroluminescence
TDPL	temperature-dependent photoluminescence
TD-TREL	temperature-dependent time-resolved electroluminescence
TD-TRPL	temperature-dependent time-resolved photoluminescence
TREL	time-resolved electroluminescence
TRPL	time-resolved photoluminescence
VE	voltage efficiency

4 LED efficiencies

4.1 General

LEDs are now found in numerous applications owing to advantages such as low power consumption, small size, long lifetime, and fast switching. LEDs are available in various spectral ranges including ultraviolet, visible, and infrared wavelengths, based on different material systems [5]-[7]. Although the LEDs have simple pn junctions with a long history of researches since the early 1960s, there still remain multiple issues in relation with the device configurations and materials. In order to analyse any possible device issues, accurate characterization of the device is essential.

Many parameters have been utilized for LED devices to quantify the device performance: parameters obtained from simple current-voltage (I-V) and light-current (L-I) measurements constitute a basis. However, they don't typically give enough details about a device under test [8]-[15]. Since many device parameters are interrelated, more extensive characterization is required to form a complete picture of any possible cause behind a problem in the device and to remedy it [16],[17]. If there is any measure implemented to remedy and enhance the device performance, it is often difficult to judge whether the intended effects have been achieved by simple checking of the output parameters such as I-V, L-I, and the emission spectrum. IEC 60747-5-6:2016 lists terminology and measuring methods of basic electrical and optical characteristics of LEDs as categorized in Table 1.

Table 1 – LED items and their measuring methods listed in IEC 60747-5-6:2016

LED Characteristics	Items	Measurement Method
Electrical	Forward voltage (V_F)	6.2
	Reverse voltage (V_R)	6.3
	Differential resistance (r_f)	6.4
	Reverse current (I_R)	6.5
	Capacitance (C_t)	6.6
Temperature	Junction temperature (T_j)	6.7
	Thermal resistance ($R_{th(j-X)}$)	6.7
Frequency	Response time	6.8
	Frequency response and cut-off frequency (f_c)	6.9
Optical	Luminous flux (Φ_V)	6.10
	Radiant power (Φ_e)	6.11
	Luminous intensity (I_V)	6.12
	Radiant intensity (I_e)	6.13
	Luminance (L_V)	6.14
Spectral	Emission spectrum, peak emission wavelength (λ_p), spectral half bandwidth ($\Delta\lambda$)	6.15
Chromatic	Chromaticity	6.16
Directional	Directivity	6.17
	Illuminance (E_V)	6.18
Quality Evaluation	Quality evaluation test and inspection	8

Of various device parameters, efficiencies contain the most important information on the device performance and any possible problem in it. IEC 60747-5-8 defines various efficiencies relevant to the LED devices. The overall efficiency of the LED device is characterized by the power efficiency (PE), η_{PE}. The PE is rather simple to measure and serves as a useful parameter representing how efficient the device is in converting the electrical power to the desired radiant power. However, in many cases, one needs to know more details than the PE to infer limiting factors in device performance.

The PE can be decomposed into its constituent factors, which are the voltage efficiency (VE), η_{VE}, and the external quantum efficiency (EQE), η_{EQE}. The EQE is then decomposed into the light extraction efficiency (LEE), η_{LEE}, and the internal quantum efficiency (IQE), η_{IQE}. The IQE is in turn separated into the injection efficiency (IE), η_{IE}, and the radiative efficiency (RE), η_{RE}. The PE, VE, and EQE are measurable by using experimental data of current, voltage, radiant power, and spectra. On the other hand, a standard method of measuring the IQE has not been known since the advent of LEDs in 1960s, before the publication of IEC 60747-5-9:2019 and 60747-5-10:2019.

The EQE is a measurable quantity once the mean photon energy is obtained. It can be limited by either the IQE or the LEE. Thus, a separate measurement of the IQE and the LEE is extremely useful not only to improve the device performance but also to elucidate the operating mechanisms of an LED device. The optimization of the epitaxial structure and the growth condition is a typical method for achieving a high IQE. A high LEE is achieved by reducing the

total internal reflection at the LED surface. The LEE and the IQE can be separately obtained from the EQE if one of them is known. In general approaches, the LEE is theoretically calculated and the IQE is experimentally measured. Theoretical calculation of the LEE is limited to specific cases in practice. This is because the LEE is very sensitive to the microscopic parameters such as the complex refractive index of each material, the layer structure, or the randomly textured surface [18]-[20]. Thus, direct measurement of the IQE as a function of current is more practical and has been pursued actively.

This technical report focuses on direct measurement methods of the IQE as a function of current in single LED chip or package without phosphor. Various characterization techniques for measuring the LED IQE are critically reviewed and compared. After the limitations of the existing IQE measurement techniques are reviewed, the room-temperature reference-point method (RTRM) is presented as a most accurate and practical IQE measurement method. The RTRM is then applied to various LED devices to show how the IQE measurement techniques can be utilized to analyse their optoelectronic performances quantitatively.

4.2 Theoretical background of optoelectronic efficiencies

Usually, an LED is electrically driven by a power supply producing the voltage V_F and the forward current I_F. The total electrical power supplied is $V_F I_F$. The LED operation is more clearly understood when $V_F I_F$ is expressed as $(qV_F)(I_F/q)$, where q is the elementary charge of 1.6x10^{-19} C: I_F/q is the total number of electrons injected into an LED per second, and qV_F is an average electrical potential energy of each electron given by the forward voltage V_F. In the ideal case, each electron energized by a power supply emits one photon without any energy loss so that both quantum particles should have the same energy qV_F. In a real case, however, there are many sorts of electrical and optical energy loss mechanisms during the electrical-to-optical energy-conversion process.

For LEDs, various efficiencies can be defined as a measure of different conversion processes [5]-[7]. The overall efficiency of an LED device can be characterized by the PE. The PE, η_{PE}, is defined as the ratio of the radiant power (coupled to the free space), Φ_e, to the input electrical power $V_F I_F$, i.e.,

$$\eta_{PE} \equiv \frac{\text{radiant power}}{\text{electrical power}} = \frac{\Phi_e}{V_F I_F} \tag{1}$$

The PE represents how efficiently an LED device can convert the electrical energy to the optical energy and thus is the most important efficiency parameter. The electrical energy that is not converted to the optical energy is wasted as heat. There are various factors that can affect the PE and these factors are characterized by various other efficiency parameters. From now on, the efficiency parameters that constitute the PE are described in detail.

The VE, η_{VE}, represents the ratio of the average photon energy emitted from the LED to the average electron energy supplied by the power source:

$$\eta_{VE} \equiv \frac{\text{mean photon energy}}{\text{mean electron energy}} = \frac{h\bar{\nu}}{qV_F}, \tag{2}$$

where $h\bar{\nu}$

and recombination process. Recently, it was also pointed out that space charges of electrons and holes accumulated near the active region also contribute additional forward voltage for a desired forward current I_F [21]-[23]. In order to improve the voltage efficiency, both low forward turn-on voltage and small series resistance are required. The VE is experimentally measurable so that the value can be improved by a sort of feedbacks to fabrication processes and LED chip designs.

The mean photon energy $h\bar{\nu}$ is defined as follows:

$$h\bar{\nu} \equiv \frac{\Phi_e}{\int_0^\infty \frac{\lambda}{hc}\Phi_{e,\lambda}(\lambda)d\lambda}, \tag{3}$$

Here, h is the Planck constant, c is the speed of light in vacuum, and λ is the free-space wavelength. Note that the integral $\int_0^\infty \frac{\lambda}{hc}\Phi_{e,\lambda}(\lambda)d\lambda$ represents the number of photons emitted from the LED per second. The average photon energy should be approximately equal to the bandgap energy of the active region of the LED.

Another is the EQE, η_{EQE}, defined as the ratio of the number of photons emitted into the free space per unit time to the number of electrons injected into the LED per unit time, i.e.,

$$\eta_{EQE} = \frac{\Phi_e/h\bar{\nu}}{I_F/q}, \tag{4}$$

where

$\Phi_e/h\bar{\nu}$ is the number of photons emitted into free space per second;

I_F/q is the number of electrons injected into LED per second.

Note from Formulae (2) and (4) that the multiplication of the VE and the EQE gives the PE, i.e.,

$$\eta_{PE} = \eta_{VE} \cdot \eta_{EQE}. \tag{5}$$

The IQE, η_{IQE}, is defined as the ratio of the number of photons emitted *from the active region* per unit time to the number of electrons injected into the LED per unit time:

$$\eta_{IQE} = \frac{\Phi_{e,active}/h\bar{\nu}}{I_F/q}, \tag{6}$$

where

$\Phi_{e,active}$ is the radiant power emitted from the active region;

$\Phi_{e,active}/h\bar{\nu}$ is the number of photons emitted from active region per second;

I_F/q is the number of electrons injected into LED per second.

The IQE is greatly dependent on crystal growth and the epitaxial layer structure. The IQE is one of the key performance indicators of LEDs.

The ratio of the number of photons emitted *into the free space* to the number of photons emitted from the active region is defined as the light extraction efficiency (LEE), η_{LEE}:

$$\eta_{LEE} = \frac{\Phi_e}{\Phi_{e,active}} . \quad (7)$$

where

Φ_e is the number of photons emitted into free space per second;

$\Phi_{e,active}$ is the radiant power emitted from the active region.

The LEE is a measure of the photon loss during the propagation from the active region into free space. In an ideal LED, all photons emitted by the active region should escape from an LED die. However, in a real LED, not all the radiant power emitted from the active region is emitted into the free space by such factors as total internal reflection. The trapped light inside the LED chip is eventually absorbed by the device, generating heat. Increasing the LEE is one of the main endeavours many chip manufactures are dedicated to so that they could improve the PE.

Using the EQE and the IQE, the LEE can be expressed as

$$\eta_{LEE} = \frac{\eta_{EQE}}{\eta_{IQE}}$$

Or

$$\eta_{EQE} = \eta_{IQE} \cdot \eta_{LEE} \quad (8)$$

The IE, η_{IE}, is defined as the ratio of the electrons injected into the active region per unit time to the number of electrons injected into the LED per unit time, expressed as

$$\eta_{IE} = \frac{I_{F,active}}{I_F} \quad (9)$$

where

$I_{F,active}$ is the number of electrons injected into active region per second;

I_F is the number of electrons injected into LED per second.

Here, $I_{F,active}$ is the portion of the forward current injected into the active region. The IE is a measure for how many electrons recombine in the active QW region compared with the total injected electrons into an LED. It depends on the current level as well as the LED structure itself. The IE is determined by nonradiative recombination rates occurring outside the active QW regions. Possible leakage currents are semiconductor surface current, defect-related tunnelling current, and electron overflow from the QW active region to p-clad region [24]-[26]. The surface leakage current is initially observed at around zero bias voltage and it shows relatively symmetric current-voltage curve for forward and reverse biases. Special surface treatment and passivation techniques have been utilized to suppress the surface leakage current. The electron blocking layer in the epitaxial growth has been introduced to reduce the electron overflow from the active region to the p-type clad layer at high-level current injection [27]. Current spreading is important to improve the current injection efficiency in terms of reducing current density over an entire LED surface. The nonuniform current injection increases

both the Joule heating and the nonradiative recombination processes and eventually lowers the light power efficiency [28],[29].

With respect to $I_{F,active}$, one can define the RE, η_{RE}:

$$\eta_{RE} = \frac{\Phi_{e,active}/h\bar{\nu}}{I_{F,active}/q}, \tag{10}$$

where

$\Phi_{e,active}/h\bar{\nu}$ is the number of photons emitted from active region per second;

$I_{F,active}/q$ is the number of electrons injected into active region per second.

which is different from the IQE by the factor IE:

$$\eta_{IQE} = \eta_{IE} \cdot \eta_{RE} \tag{11}$$

For a high RE, it is necessary to increase the radiative recombination rate and decrease the nonradiative recombination rate.

Lastly, the active efficiency (AE), η_{AE}, can be defined as the ratio of the radiant power emitted *from the active region* to the electrical power supplied to the LED:

$$\eta_{AE} = \frac{\Phi_{e,active}}{V_F I_F}, \tag{12}$$

where

$\Phi_{e,active}$ is the radiant power emitted from the active region;

$V_F I_F$ is the electric power.

which is different from the IQE in that the active region is analysed in a view of the power rather than the particle rate. The AE is a concept similar to the responsivity in a photodiode.

In summary, the overall PE can be rewritten as follows:

$$\begin{aligned} \eta_{PE} &= \eta_{VE} \cdot \eta_{EQE} \\ &= \eta_{VE} \cdot \eta_{IQE} \cdot \eta_{LEE} \\ &= \eta_{VE} \cdot \eta_{IE} \cdot \eta_{RE} \cdot \eta_{LEE} \\ &= \eta_{AE} \cdot \eta_{LEE} \end{aligned} \tag{13}$$

Or put in differently,

$$\begin{aligned} \eta_{PE} &= \frac{\Phi_e}{V_F I_F} \\ &= \frac{h\bar{\nu}}{qV_F} \cdot \frac{I_{F,active}}{I_F} \cdot \frac{\Phi_{e,active}/h\bar{\nu}}{I_{F,active}/q} \cdot \frac{\Phi_e}{\Phi_{e,active}} \end{aligned} \tag{14}$$

The efficiency definitions are summarized in Table 2.

Table 2 – Summary of efficiency items defined in IEC 60747-5-8:2019

Items	Definitions
Power efficiency (PE)	$\eta_{PE} = \frac{\Phi_e}{V_F I_F}$, where Φ_e is the radiant power; $V_F I_F$ is the electrical power.
Voltage efficiency (VE)	$\eta_{VE} = \frac{h\bar{\nu}}{qV_F}$, where $h\bar{\nu}$ is the mean photon energy; qV_F is the mean electron energy. $h\bar{\nu} \equiv \frac{\Phi_e}{\int_0^\infty \frac{\lambda}{hc}\Phi_{e,\lambda}d\lambda}$
External quantum efficiency (EQE)	$\eta_{EQE} = \frac{\Phi_{e,active}/h\bar{\nu}}{I_F/q}$, where $\Phi_e/h\bar{\nu}$ is the number of photons emitted into free space per second; I_F/q is the number of electrons injected into LED per second.
Internal quantum efficiency (IQE)	$\eta_{IQE} = \frac{\Phi_{e,active}/h\bar{\nu}}{I_F/q}$, where $\Phi_{e,active}/h\bar{\nu}$ is the number of photons emitted from active region per second; I_F/q is the number of electrons injected into LED per second.
Light extraction efficiency (LEE)	$\eta_{LEE} = \frac{\Phi_e}{\Phi_{e,active}}$ where Φ_e is the number of photons emitted into free space per second; $\Phi_{e,active}$ is the number of photons emitted from active region per second.
Injection efficiency (IE)	$\eta_{IE} = \frac{I_{F,active}}{I_F}$, where $I_{F,active}$ is the number of electrons injected into active region per second; I_F is the number of electons injected into LED per second.

Items	Definitions
Radiative efficiency (RE)	$\eta_{RE} = \dfrac{\Phi_{e,active}/h\bar{\nu}}{I_{F,active}/q}$ where $\Phi_{e,active}/h\bar{\nu}$ is the number of photons emitted from active region per second; $I_{F,active}/q$ is the number of electrons injected into active region per second.

4.3 Separate measurement of various efficiencies

The PE can be obtained in a straight-forward way by using Equation (1). Measuring the radiant power Φ_e and electrical V_F and I_F is already defined in IEC 60747-5-6:2016 (see Table 1). In order to define the EQE, one needs to find the mean photon energy $h\bar{\nu}$, using Equation (3). Once the mean photon energy is obtained, the EQE can be obtained by Equation (4). Using the obtained PE and EQE, the VE can now be calculated by using Equation (5) as $\eta_{VE} = \eta_{PE}/\eta_{EQE}$.

To separate the efficiencies further, the IQE is required. Methods of obtaining the IQE are discussed in detail in the following sections. Once the IQE is determined by a method such as the RTRM, the LEE can now be obtained by using Equation (8): $\eta_{LEE} = \eta_{EQE}/\eta_{IQE}$.

The sequence of the efficiency measurements is summarized in Figure 1.

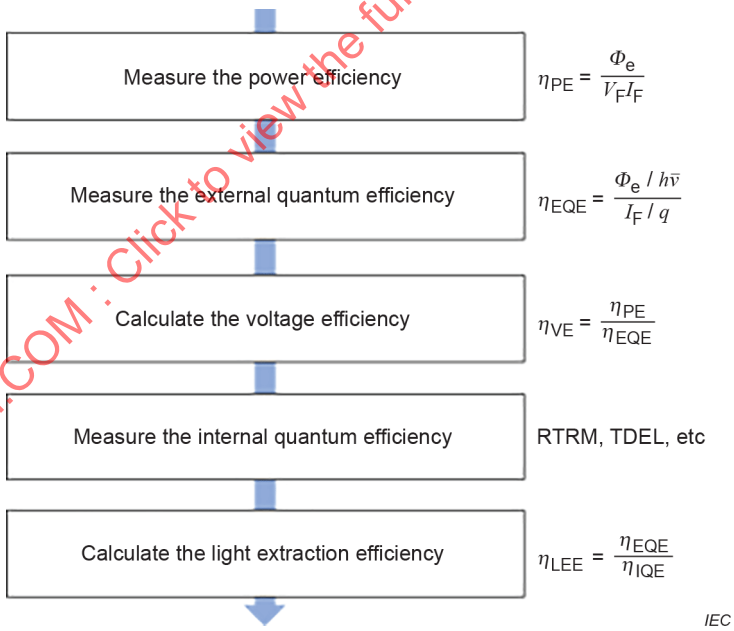

Figure 1 – Sequence of the efficiency measurements

4.4 Requirements for accurate and reliable IQE measurement

The IQE of an LED is a key parameter that represents the quality of epitaxial layers and contains essential information on operational mechanisms. Furthermore, knowing the IQE allows quantitative measurements of various efficiencies defined for LEDs. As seen in Table 2, the IQE, defined as the ratio of the number of internally emitted photons to the number of electrically injected (or optically generated) carriers, is the product of the IE and the RE. The IQE varies with the operating conditions of forward injection current I_F and temperature T as expressed below:

$$\eta_{IQE}(I_F,T) = \eta_{IE}(I_F,T)\cdot\eta_{RE}(I_F,T) \quad (15)$$

The IE is a measure of how many electrons recombine in the active region compared to the total electrons injected into an LED. It generally depends on the current level as well as the LED structure itself. The RE represents the ratio of the radiative recombination rate to the total recombination rate (i.e., the sum of the radiative and nonradiative recombination rates) in the active region. For an accurate estimation of the IQE, it is necessary to consider the IE and the RE separately and quantitatively.

The IQE measurement methods satisfying the following requirements are very desirable in view of accuracy, simplicity, reproducibility, and experimental-system cost: (i) Use only experimentally measurable physical quantities such as current and radiant power (optical power) *without* assuming any physical parameters, e.g., chip sizes, epitaxial layer structures, carrier recombination rates, and complex refractive indices; (ii) Measure the *relative* radiant power rather than the *absolute* radiant power to reduce measurement errors; (iii) Use measurement conditions of the *operational* temperature and pumping scheme. The electroluminescence (EL) at room temperature is the most preferable combination compared with others; Finally, (iv) use CW pumping and its steady-state response of the spontaneous emission, which eliminates the need for complicated and expensive experimental setups such as a short-pulse current driver, a high-speed photodetector, and an impedance matching technique for a good RF signal integrity.

In Clauses 5 and 6, the IQE measurement methods that have been frequently utilized up to now are reviewed. The technical limitations involved in these methods are compared and discussed. In order to overcome such limitations and satisfy the aforementioned requirements, a unique method of the IQE measurement, named as the room-temperature reference-point method (RTRM), has been proposed recently. The RTRM is described separately in detail.

4.5 Classification of IQE measurement methods

The discrete and accurate measurement of the LED IQE as a function of optical pumping power, injection current, or carrier density has been a constant challenge. The IQE measurement can be done theoretically or experimentally. The theoretical approach is based on calculation of the LEE and the experimental approaches utilize the EQE data measured at various conditions. Different measurement methods of the IQE as a function of input pumping rate have been reported so far as summarized in Table 3. The IQE measurement methods are named differently according to the input pumping scheme, the output temporal responses, and the sample temperatures. There are two input pumping schemes: one is the optical pumping with a laser and the other is the electrical pumping by the current. Their respective output spontaneous emissions are known as the photoluminescence (PL) and the electroluminescence (EL). The laser light intensity and electrical current are usually varied in order to change the input pumping rate. In time scale, the input pumping signal and its optical response can be either continuous wave (CW) or short-pulse trains. Sometimes sample temperatures can be varied from the cryogenic temperatures to room temperature. Each IQE measurement method in Table 3 is named to represent the input pumping scheme, temporal response, and sample temperature.

The IQE measurement methods can be largely divided into five categories: (i) calculation of the LEE, (ii) PL methods, (iii) EL methods, (iv) temperature-dependent (TD) methods, and (iv) time-resolved (TR) methods. Each method has its own pros/cons, features, and limitations in applications. Each method is described in the next section.

Table 3 – Various LED IQE measurement methods

Theoretical	Calculation of the LEE						
Experimental	Type		Pumping variable	Time scale		Sample temperature	
				CW	Dynamic	Fixed	Varied
	Pumping method	Optical	Laser intensity	PL	TRPL	PL,TRPL	TDPL, TD-TRPL
		Electrical	Current	EL	TREL	EL,TREL	TDEL, TD-TREL
CW: continuous wave; PL: photoluminescence; EL: Electroluminescence; TR: time-resolved; TD: temperature-dependent; and RTRM: room-temperature reference-point method							

5 Conventional IQE measurement methods: features and limitations

5.1 Calculation of the LEE

The method based on calculation of the LEE [category (i) in 4.5] indirectly measures the IQE by dividing the measured EQE with the calculated LEE. Thus, it requires both the accurate measurement of the absolute radiant power and the precise knowledge of model parameters for LEE calculation. This method has been frequently applied due to its simplicity. But unwanted errors can be easily involved in calculation due to unclear model parameters such as chip shape and dimensions, fine textured structures in chip surfaces or substrate, epitaxial structures and their material constants, e.g., complex refractive indices [30]-[41]. This method is almost impossible to use without knowing the detailed structure and operating conditions. Therefore, there are limitations to adopting this method as an international standard for measuring the IQE of any LED chips. It is preferable to measure the IQE of an LED chip only from the stably obtainable experimental data.

5.2 Temperature-dependent photoluminescence (TDPL)

The PL methods [category (ii) in 4.5] are nondestructive and the IQE of the active layers can be evaluated on an epitaxial wafer without fabricating the actual devices. The most popularly utilized IQE measurement method based on the PL is the continuous-wave (CW) temperature-dependent photoluminescence (TDPL) method [42]-[57].

An advantage of TDPL is that the IQE (η_{IQE}) can be directly determined experimentally without the aid of any calculations or physical-parameter assumptions.

Experimentally the PL efficiency (η_{PL}) is defined by the ratio of the integrated PL intensity (I_{PL}) to the laser excitation intensity (I_{laser}), i.e. $\eta_{\mathrm{PL}} = I_{\mathrm{PL}}/I_{\mathrm{laser}}$. Sometimes, η_{PL} is normalized to its peak value among all experimental data. In the TDPL, it is considered that $\eta_{\mathrm{PL}}\left(T, I_{\mathrm{laser}}\right)$ is linearly proportional to $\eta_{\mathrm{IQE}}\left(T, I_{\mathrm{laser}}\right)$ and the LEE (η_{LEE}) is independent of temperature and laser excitation intensity. In addition, the IQE is assumed as 100 % at the maximum PL efficiency for various experimental conditions of environmental temperatures and laser excitation intensities, i.e. $\eta_{\mathrm{IQE}}\left(T_{\mathrm{low}}, I_{\mathrm{laser,max}}\right) = 100\ \%$.

Following these assumptions, the IQEs from the experimental PL efficiencies measured at various temperatures and laser intensities are obtained. Usually, the maximum PL efficiency ($\eta_{\mathrm{PL,max}}$) is found at a cryogenic temperature (T_{low}) and a certain excitation level ($I_{\mathrm{laser,max}}$). Then, $\eta_{\mathrm{IQE}}\left(T, I_{\mathrm{laser}}\right)$ is calculated by

$$\eta_{\mathrm{IQE}}\left(T, I_{\mathrm{laser}}\right)\Big|_{\mathrm{TDPL}} = \frac{\eta_{\mathrm{PL}}\left(T, I_{\mathrm{laser}}\right)}{\eta_{\mathrm{PL,max}}\left(T_{\mathrm{low}}, I_{\mathrm{laser,max}}\right)}. \tag{16}$$

In order to apply Equation (16), it is necessary to confirm $\eta_{\mathrm{IQE}}\left(T_{\mathrm{low}}, I_{\mathrm{laser,max}}\right) = 100\ \%$ satisfying IE = RE = 100 % at the maximum PL efficiency ($\eta_{\mathrm{PL,max}}$). One of the informative methods investigating the carrier recombination processes only in the QW active layers is the resonant PL. In the resonant PL, the photon energy of the optical pumping source is between the bandgap energy of the well and that of the barrier to selectively excite the carriers only in the QWs. This is intended to eliminate the influence of carries excited and transported in regions other than the active layer. According to this idea, it is generally assumed that IE = 100 %, i.e., all the carriers generated in the active layers recombine there. However, in contrast to this assumption, it has been reported experimentally that the carrier escape from the QWs does take place with a strong dependence on the duration of excitation and bias conditions [57].

A technique confirming the IE of 100 % in the resonant PL has been proposed, which is comparing three characteristics, i.e., the PL efficiency and the open-circuit voltage in the resonant PL experiment and the EL efficiency in the EL experiment. It was experimentally reported that the efficiency droop behaviours of a 440-nm InGaN-based blue LED as functions of temperature and pumping level were quite similar in both the resonant PL and EL experiments [55]. This observation strongly indicates that the carrier spill-over or carrier overflow from the QWs due to limited carrier recombination rates inside the QWs is considered as an important origin of the efficiency droop in both the resonant PL and EL experiments. As a result, it should be remembered that carrier overflow is possible even at the resonant PL experiments, resulting in IE < 100 %.

To find the reference point satisfying RE = 100 %, the second assumption is used. At cryogenic temperatures, the nonradiative recombination centres in the active layers, which induce the Shockley-Read-Hall (SRH) recombination, are "frozen" and become inactive. Moreover, the direct Auger recombination rate in conventional semiconductors decreases exponentially with decreasing temperature so that the contribution of the Auger recombination rate can also be neglected at the reference point. By assuming that both the SRH and Auger recombination rates are negligibly small at cryogenic temperatures, the RE is considered as 100 % [43],[44]. In experiments, the assumption of RE = 100 % is confirmed from the fact that the peak EQEs at cryogenic temperatures do not increase further and maintain the maximum value with decreasing temperatures. On the other hand, the assumption of IE = 100 % is experimentally confirmed from the fact that the peak PL efficiencies where the RE is considered as 100 % do not vary and maintain the maximum value with pumping laser intensity.

However, in many cases, it has been reported that the laser intensity is changed at a specific cryogenic temperature or vice versa [45]. It should be remembered that these experiments cannot be used for the IQE measurement because the IE and the RE cannot be guaranteed as 100 % simultaneously at the maximum PL efficiency.

5.3 Intensity-dependent photoluminescence (IDPL) or simply photoluminescence (PL)

Another method based on the PL at room temperature for determining the IQEs has been reported by fitting the laser pump intensity to powers of the integrated PL intensity. This is named as the intensity-dependent photoluminescence (IDPL) or simply the PL in Table 3 [58]-[61]. In the IDPL or PL method, the well-known constant ABC model for the carrier rate equation is theoretically utilized.

The dependence of the PL intensity on the laser pump power is formulated by using photon and carrier rate equations in the active layer with the assumption that both the optical absorption coefficient of the pump laser light and the carrier recombination coefficients are independent of the laser pump power or the carrier density there. In addition, it is implicitly assumed that the IE is constant (a value of either one or less than one). This implies that all or a constant

percentage of carriers generated in the active layers recombine there. The theoretical background of the IDPL is described next.

The rate equation of the carrier density $n(t)$ in the active QW is written by the relationship between the carrier injection rate G_{inj} and the total recombination rate R as follows:

$$\frac{dn}{dt} = G_{\text{inj}} - R \tag{17}$$

A laser pumping with the total generation rate of G is considered. Then, a part of the total generated carriers in the active layers are recaptured and recombine there, which is the IE, η_{IE}:

$$G_{\text{inj}} = \eta_{\text{IE}} G \,. \tag{18}$$

The total generation rate G is given by

$$G = \left(1 - R_{\text{surface}}\right) \frac{\alpha l P_{\text{laser}}}{A_{\text{spot}} l h\nu_{\text{L}}} = \frac{\left(1 - R_{\text{surface}}\right)\alpha}{A_{\text{spot}}} \frac{P_{\text{laser}}}{h\nu_{\text{L}}}, \tag{19}$$

where R_{surface}, α, $h\nu_{\text{L}}$, and P_{laser} are the reflectivity on the semiconductor surface, the absorption coefficient in the active QWs, the photon energy, and the excitation laser power, respectively [61].

According to the well-known constant-ABC model, there are three main recombination mechanisms, namely, the nonradiative SRH recombination, the radiative recombination, and the Auger recombination, the recombination rates of which are proportional to n, n^2, and n^3, respectively:

$$R = An + Bn^2 + Cn^3 \,, \tag{20}$$

where A, B, and C are the recombination coefficients representing the SRH, radiative, and Auger recombinations, respectively.

At a steady state where $dn/dt = 0$ in Equation (17), the carrier injection rate is the same as the recombination rate, i.e., $G_{\text{inj}} = \eta_{\text{IE}} G = R$. Then, Equations (18), (19) and (20) lead to the following:

$$\frac{P_{\text{laser}}}{h\nu_{\text{L}}} = \frac{A_{\text{spot}}}{\eta_{\text{IE}}\left(1 - R_{\text{surface}}\right)\alpha}\left(An + Bn^2 + Cn^3\right) = \frac{1}{\eta_{\text{IE}}\eta_{\text{L}}}\left(An + Bn^2 + Cn^3\right), \tag{21}$$

where $\eta_{\text{L}} = \left(1 - R_{\text{surface}}\right)\alpha / A_{\text{spot}}$. The integrated PL power (P_{PL}) over the wavelength is detected by a photodetector and is given by

$$\frac{P_{\text{PL}}}{h\bar{\nu}} = \left(\eta_{\text{det}}\eta_{\text{LEE}} V_{\text{active}}\right) Bn^2 = \eta_{\text{D}} Bn^2 \,, \tag{22}$$

where $\eta_D = \eta_{det}\eta_{LEE}V_{active}$. η_{det} and V_{active} are the total detector coupling efficiency and the active volume, respectively.

The RE (η_{RE}) is given by the radiative recombination rate over the total carrier recombination rate in the active layers and the IQE (η_{IQE}) is obtained by the radiative recombination rate to the total generation rate (G):

$$\eta_{RE} = \frac{Bn^2}{G_{inj}} = \frac{Bn^2}{R} = \frac{Bn^2}{An + Bn^2 + Cn^3}; \tag{23}$$

$$\eta_{IQE} = \frac{Bn^2}{G} = \eta_{IE}\frac{Bn^2}{G_{inj}} = \eta_{IE}\frac{Bn^2}{R} = \eta_{IE}\frac{Bn^2}{An + Bn^2 + Cn^3} = \eta_{IE}\eta_{RE}. \tag{24}$$

The PL efficiency (η_{PL}) is defined as the ratio of the radiative photon rate to the excitation laser photon rate:

$$\eta_{PL} = \frac{P_{PL}/h\bar{\nu}}{P_{laser}/h\nu_L} = \frac{\eta_{IE}\left(1 - R_{surface}\right)\alpha_L\left(\eta_c\eta_{LEE}V_{active}\right)Bn^2}{A_{spot}\left(An + Bn^2 + Cn^3\right)} = \eta_{IE}\eta_L\eta_D\frac{Bn^2}{An + Bn^2 + Cn^3} \tag{25}$$
$$= \eta_L\eta_D\eta_{IE}\eta_{RE} = \eta_L\eta_D\eta_{IQE}$$

From Equation (25), it can be seen that η_{PL} is not equal but linearly proportional to η_{IQE}. In order to find an exact value of η_{IQE}, it is necessary to know η_{IE} and η_{RE} separately.

Next, the experimental values of the laser intensity are theoretically related to the PL intensity. From Equation (22), the carrier density n in the active layer is expressed by the PL intensity:

$$n = \frac{1}{\sqrt{\left(\eta_D B\right)h\bar{\nu}}}\sqrt{P_{PL}}. \tag{26}$$

The laser intensity P_{laser} in Equation (21) can be rewritten by

$$P_{laser} = \frac{h\nu_L}{\eta_{IE}\eta_L}R = \frac{h\nu_L}{\eta_{IE}\eta_L}\left(An + Bn^2 + Cn^3\right)$$
$$= \frac{h\nu_L}{\eta_{IE}\eta_L}\frac{A}{\sqrt{\left(\eta_D B\right)h\bar{\nu}}}\sqrt{P_{PL}} + \frac{h\nu_L}{\eta_{IE}\eta_L}\frac{1}{\left(\eta_D\right)h\bar{\nu}}\left(\sqrt{P_{PL}}\right)^2 + \frac{h\nu_L}{\eta_{IE}\eta_L}\frac{C}{\sqrt{\left(\eta_D B\right)^3\left(h\bar{\nu}\right)^3}}\left(\sqrt{P_{PL}}\right)^3 \tag{27}$$
$$= P_1\sqrt{P_{PL}} + P_2\left(\sqrt{P_{PL}}\right)^2 + P_3\left(\sqrt{P_{PL}}\right)^3$$

where

$$P_1 = \frac{h\nu_L}{\eta_{IE}\eta_L}\frac{A}{\sqrt{\left(\eta_D B\right)h\bar{\nu}}},\ P_2 = \frac{h\nu_L}{\eta_{IE}\eta_L}\frac{1}{\left(\eta_D\right)h\bar{\nu}},\ P_3 = \frac{h\nu_L}{\eta_{IE}\eta_L}\frac{C}{\sqrt{\left(\eta_D B\right)^3\left(h\bar{\nu}\right)^3}}. \tag{28}$$

Then, η_{RE} in Equation (23) can be expressed by using Equation (27) as

$$\eta_{RE} = \frac{Bn^2}{An + Bn^2 + Cn^3} = \frac{P_2\left(\sqrt{P_{PL}}\right)^2}{P_1\sqrt{P_{PL}} + P_2\left(\sqrt{P_{PL}}\right)^2 + P_3\left(\sqrt{P_{PL}}\right)^3}. \tag{29}$$

As a result,

$$\eta_{IQE} = \eta_{IE}\eta_{RE} = \eta_{IE}\frac{P_2\left(\sqrt{P_{PL}}\right)^2}{P_1\sqrt{P_{PL}} + P_2\left(\sqrt{P_{PL}}\right)^2 + P_3\left(\sqrt{P_{PL}}\right)^3}. \tag{30}$$

It is expected from Equation (26) that P_{laser} can be expressed by the power-dependence of $\sqrt{P_{PL}}$ with P_1, P_2, and P_3 as constant fitting parameters. In fact, many parameters in P_1, P_2, and P_3 may be dependent on the laser power P_{laser}. There have been many reports on the carrier-density dependent characteristics of η_{IE}, A, B, C, α, and η_{LEE}. Thus, it should be noted that the constant fitting parameters P_i be much slowly varying with $\sqrt{P_{PL}}$. After the fitting process, η_{RE} can be calculated as a function of P_{laser} from Equation (29). Once the IE is known, then the IQE can be calculated from Equation (30).

In the fitting process, it is implicitly assumed that the IE is constant (approximately 1). As a result, the RE is equal to be the IQE and the PL efficiency degradation at high pumping rates is due to the Auger nonradiative recombination process. However, it is not clear whether the increase in the Auger nonradiative recombination rate or the decrease in the IE is the origin of the IQE degradation at high pumping rates. As a result, these assumptions make it difficult to evaluate the IQE with the PL method. On the other hand, it is expected that the IDPL (or simply PL) method would be very helpful to estimate the active-layer quality as high radiative recombination rate.

5.4 Temperature-dependent time-resolved photoluminescence (TD-TRPL)

The time-resolved photoluminescence (TRPL) measurement, an observation of the temporal response of the PL, has been known as a useful experimental tool to study new materials [62]-[76]. This is because the temporal information combined with the spectral data can help determine the carrier dynamics involved in optical processes such as the lifetimes of minority carriers, free and bound excitons, localized excitons, and tunnelling. The temperature-dependent time-resolved photoluminescence (TD-TRPL) method has been widely used to determine the radiative and nonradiative carrier lifetimes separately in conjunction with the measured IQE values. In the TD-TRPL method, measurement of the IQE follows the same procedure as the TDPL method previously explained.

The transient luminescence intensity $I(T,t)$ obtained by the data of TRPL is analysed by using the carrier rate equation in the active layer. As a very rough approximation, it is assumed that all carriers generated in the active layers recombine there (i.e., IE = 100 %). Moreover, the radiative carrier lifetime $\tau_r(T)$ and nonradiative carrier lifetime $\tau_{nr}(T)$ are usually assumed to be constant independent of carrier density n in the active layer. Then, the carrier rate equation just after the laser pulse is turned off $\left(t = 0^+\right)$ and its solution is obtained as follows:

$$\frac{dn}{dt} = -\frac{n}{\tau} = -n\left(\frac{1}{\tau_r} + \frac{1}{\tau_{nr}}\right);$$
$$n(T) = n_o(T)\exp\left(-\frac{t}{\tau(T)}\right), \quad . \tag{31}$$

where $\frac{1}{\tau(T)} = \frac{1}{\tau_r(T)} + \frac{1}{\tau_{nr}(T)}$ for $t \geq 0^+$.

Then,

$$I_{PL}(T,t) = C_c \frac{n}{\tau_r} = I_{PL,o}(T)\exp\left(-2\frac{t}{\tau(T)}\right) = I_{PL,o}(T)\exp\left(-\frac{t}{\tau_{PL}(T)}\right) \tag{32}$$

where $I_{PL,o}(T) = C_c \frac{n_o(T)}{\tau_r(T)}$ and $\tau(T) = 2\tau_{PL}(T)$.

In Equation (32), $I_{PL,o}(T)$ is the peak PL intensity at t = 0+ integrated over the whole emission spectrum and $\tau_{PL}(T)$ is the decay time of the PL intensity at a given temperature (T in K). Experimentally, the transient luminescence intensity $I(T,t)$ of the TRPL is fitted to Equation (32) and $\tau_{PL}(T)$ is obtained from its initial slope in time.

Once the IQE is known, then the radiative and nonradiative carrier lifetimes can be measured separately. The IQE in the TD-TRPL is obtained from a procedure quite similar to that of the TDPL shown in 6.2. The pulse width used in the TRPL is so short that all the generated carriers are fallen into the quasi-equilibrium state before starting the recombination. Then, the PL efficiency (η_{PL}) is defined by $\eta_{PL} = I_{PL,o}/I_{laser}$ by using $I_{PL,o}(T)$ in Equation (32). As in TDPL, the IQE is assumed as 100 % at the peak PL efficiency showing a constant value at certain range of low temperature (T_{low}) and laser excitation intensity $(I_{laser,max})$, i.e., $\eta_{IQE}(T_{low}, I_{laser,max}) = 100$ %. Then, $\eta_{IQE}(T, I_{laser})$ at any temperature T and laser excitation intensity is calculated by Equation (16), i.e., $\eta_{IQE}(T, I_{laser})|_{TDPL} = \eta_{PL}(T, I_{laser})/\eta_{PL,max}(T_{low}, I_{laser,max})$. Then, the radiative and nonradiative carrier lifetimes are measured separately from

$$\eta_{IQE}(T) = \frac{1/\tau_r}{1/\tau_r + 1/\tau_{nr}}; \tag{33}$$

$$\tau_r(T) = \frac{2\tau_{PL}}{\eta_{IQE}} \text{ and } \tau_{nr}(T) = \frac{2\tau_{PL}}{1-\eta_{IQE}}. \tag{34}$$

In summary, the TRPL measurement is a very useful tool to investigate the radiative and nonradiative recombination processes in semiconductor materials. The analysis of the temporal response of the luminescent intensity measured from various conditions of laser excitation intensities and sample temperatures makes it possible to know the radiative and nonradiative carrier lifetimes separately at room temperature. In the TD-TRPL, the IQE is separately measured from a similar procedure applied to the TDPL. Then, the measured PL decay time is

resolved to the radiative and nonradiative carrier lifetimes by combining the IQE with the PL decay time. There are too many cases that the assumptions of the IE = 100 % and constant carrier lifetimes are not appropriate. It should be checked in each case before applying the aforementioned method.

5.5 Time-resolved photoluminescence (TRPL)

For practical IQE measurements, the IQE can be measured at room temperature where LEDs are actually operating. A method of measuring both the carrier lifetime and the IQE at the same time was reported by analysing the TRPL response at room temperature [77], [78]. The analysis is theoretically based on the carrier rate equation. In order to measure the IQE from the TD-TRPL method, the TRPL response has to be measured repeatedly at various temperatures as previously described, which requires a significant amount of measuring time and complicated experimental setups.

The TRPL measurement utilizes short pulse trains from a photoexcitation source, whose single pulse width is approximately a few hundred femtoseconds to a few picoseconds, and the pulse period is long enough to measure the single pulse response without inter-symbol interference. After a short optical pulse illumination, the electrons and holes are excited in the conduction and valence bands, respectively, and are redistributed close to the band edges in the intraband relaxation time of less than a few hundred femtoseconds, which is known as the quasi-equilibrium distributions. The redistributed electrons start to lose energy within a few nanoseconds to a hundred nanoseconds by recombining with holes to generate photons, or with material defects to produce heat. Therefore, the optical pulse can be considered as a pump light source, with the same amplitude of the optical pulse, with a time-averaged optical power (P_{pump}) as shown in Figure 2 a).

Furthermore, the density of free carriers in the conduction band can be assumed to be initially pumped to the steady state n_0 by P_{pump}, and the recombination processes begin just after the pulse has been turned off ($t = 0^+$) as in Figure 2 b). Here, P_{pump} is assumed to be sufficiently high so that the recombination of excitons can be ignored. The rate equation of the carrier density $n(t)$ in the active layer can be written as

$$\frac{dn}{dt} = \eta_{\text{IE}} G - \frac{n}{\tau} = \eta_{\text{IE}} \frac{(1 - R_{\text{surface}})\alpha}{A_{\text{spot}} h\nu_{\text{L}}} P_{\text{laser}} - \left(An + Bn^2 + Cn^3 \right); \tag{35}$$

$$\frac{1}{\tau_{\text{s}}} = \frac{1}{\tau_{\text{r}}} + \frac{1}{\tau_{\text{nr}}} = A + Bn + Cn^2, \tag{36}$$

where η_{IE}, R_{surface}, α, $h\nu_{\text{L}}$, and P_{pump} in Equation (35) are the IE, the reflectivity on the semiconductor surface, the absorption coefficient in the active layers, the photon energy, and the excitation laser power, respectively. τ_{s} is the carrier lifetime at the static state, which can be separated into the nonradiative recombination carrier lifetime (τ_{nr}), and the radiative recombination carrier lifetime (τ_{r}). A, B, and C in Equation (36) are recombination coefficients representing the SRH, radiative, and Auger recombinations, respectively.

Since the spontaneous light emission from an LED in Figure 2 c) is proportional to the radiative recombination, the detected amount of light power $P_{\text{PL}}(t)$ is given by

$$P_{\mathrm{PL}}(t) = \left(h\bar{\nu}\eta_{\mathrm{det}}\eta_{\mathrm{LEE}}V_{\mathrm{active}}\right)Bn^2 = \eta_{\mathrm{c}}Bn^2 = \eta_{\mathrm{c}}\left(\frac{n}{\tau_{\mathrm{r}}}\right) \tag{37}$$

where $\eta_{\mathrm{c}} = \eta_{\mathrm{det}}\eta_{\mathrm{LEE}}h\bar{\nu}V_{\mathrm{active}}$. η_{det} , η_{LEE} , $h\bar{\nu}$, and V_{active} are the total detector coupling efficiency, the LEE, the mean photon energy, and the active volume, respectively.

Here, the Auger recombination process is neglected for simplicity. The Auger recombination rate is proportional to the cube of carrier density (Cn^3) and can be important at high laser pump powers. For laser powers far below the laser power at the peak PL efficiency, the Auger recombination can be negligible. In usual TRPL measurements, the incident power density from a pump laser diode is as weak as a few W/cm^2, which corresponds to a current density of sub A/cm^2 in forward current injection. At this current density, the Auger recombination rate is expected to be much smaller compared to the radiative recombination rate.

For t > 0, the optical excitation is absent. Thus, the carrier rate equation is written as

$$\frac{dn}{dt} = -\left(An + Bn^2\right), \tag{38}$$

where $n(t) = n_0 + \Delta n(t)$. Here, $n(t)$ represents the time-dependent variation of the carrier density when $t \geq 0$ and n_0 is the carrier density when $t < 0$. Then, the following differential equation for $n(t)$ is obtained:

$$\frac{d(\Delta n)}{dt} = -(An_0 + Bn_0^2) - (A + 2Bn_0)\Delta n - B(\Delta n)^2 . \tag{39}$$

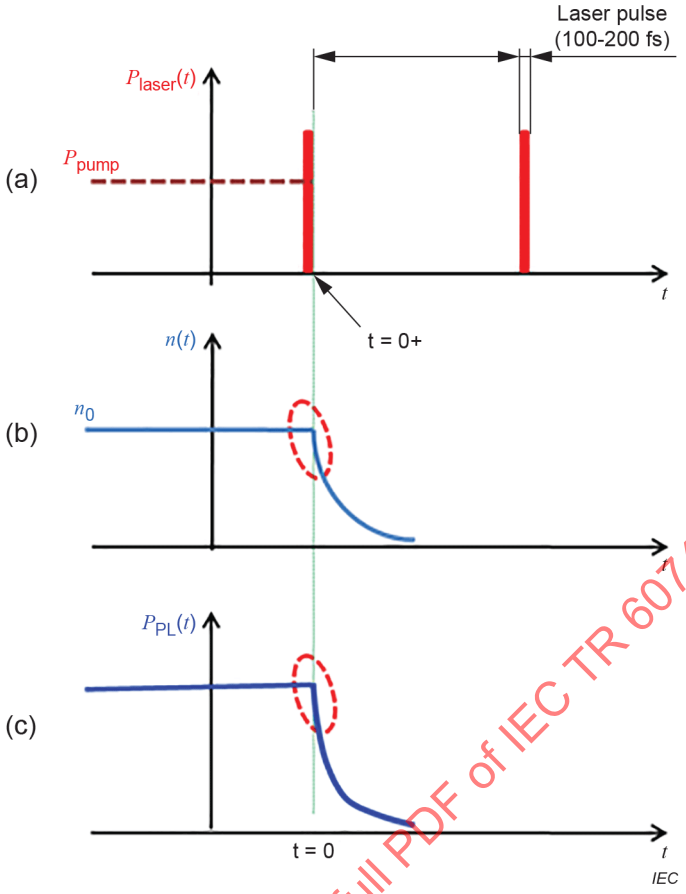

Figure 2 – Theoretical model for analysing the TRPL experiment

The general solution for Equation (39) is given by

$$\Delta n(t) = -\frac{A + 2Bn_0}{2B} + \frac{A}{2B}\frac{1 + Ke^{-At}}{1 - Ke^{-At}}, \tag{40}$$

where K is an arbitrary constant. The arbitrary constant K can be found from the initial condition, where $\Delta n(0) = 0$, which is solved as

$$K = \frac{Bn_0^2}{An_0 + Bn_0^2}. \tag{41}$$

The coefficient K happens to be the same as the definition of IQE when $t < 0$. To check the validity of Equations (40) and (41), the physical condition of $\Delta n(\infty) = -n_0$ can be shown to be satisfied for self-consistency. Therefore, the time dependent carrier density $n(t)$ is finally obtained to be

$$n(t) = \frac{A}{B}\frac{\eta_{IQE}\, e^{-At}}{1 - \eta_{IQE}\, e^{-At}}. \tag{42}$$

Furthermore, the detected radiant power can be calculated from Equations (37), (41), and (42). The detected radiant power normalized with its maximum ($P_{PL}(t=0) = \eta_c B_0 n_0^2$) is given by

$$P_{\text{nor}}(t) = \left(\frac{A}{Bn_0}\right)^2 \frac{\eta_{\text{IQE}}^2 \, \text{e}^{-2At}}{\left(1 - \eta_{\text{IQE}} \, \text{e}^{-At}\right)^2} . \tag{43}$$

$P_{\text{nor}}(t)$ derived above is more complicated than a simple single exponential function with time. However, it can be approximated as a single exponential function at the initial and final stages, i.e.,

$$P_{\text{nor}}(t) \approx e^{-t/\tau_{\text{PL,initial}}} \qquad \text{as } t \to 0 ; \tag{44}$$

$$P_{\text{nor}}(t) \approx \left(\frac{A}{A + Bn_0}\right)^2 e^{-t/\tau_{\text{PL,final}}} \qquad \text{as } t \to \infty . \tag{45}$$

In Equations (44) and (45), each lifetime is given as

$$\frac{1}{\tau_{\text{PL,initial}}} = 2\left(A + Bn_0\right) = 2\left(\frac{1}{\tau_{\text{nr}}} + \frac{1}{\tau_{\text{r}}}\right). \tag{46}$$

$$\frac{1}{\tau_{\text{PL,final}}} \approx 2A = \frac{2}{\tau_{\text{nr}}} . \tag{47}$$

Note that at $t = 0^+$, $\tau_{\text{PL,initial}}$ is one half of the carrier lifetime τ defined in Equation (36). On the other hand, for the case of the final stage in the TRPL response ($t >> \tau_{\text{PL,initial}}$), $\tau_{\text{PL,final}}$ can be approximately given only in terms of the nonradiative recombination coefficient. The nonradiative carrier lifetime τ_{nr} is twice the carrier lifetime of the final stage in the TRPL response ($\tau_{\text{PL,final}}$). Equations (46) and (47) mean that both the radiative and nonradiative recombination processes determine the lifetime of the TRPL response at the initial stage, whereas the nonradiative recombination process mainly determines the lifetime at the final stage. This can be understood as both the radiative and nonradiative recombination processes compete with each other at the initial stage in the PL decay when the radiant power is high. As time progresses to the final stage in the PL decay, most of the radiative recombination process has taken place, and the PL decay curve is mainly governed by the nonradiative recombination lifetime.

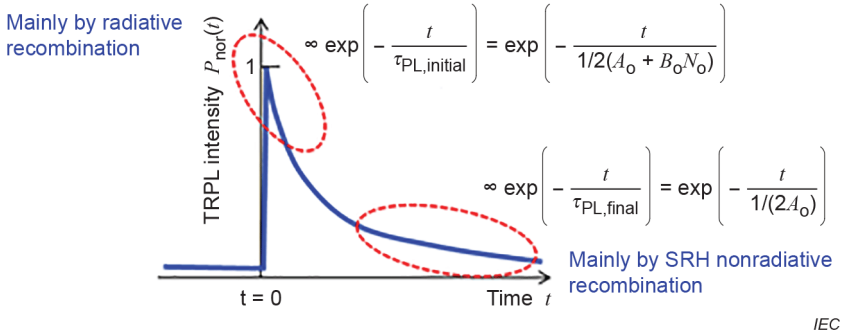

Figure 3 – Schematic TRPL response and its interpretation in terms of various lifetimes

From Equations (46) and (47), the IQE (η_{IQE}) and the radiative recombination carrier lifetime (τ_r) can be obtained directly from the measured $\tau_{PL,initial}$ and $\tau_{PL,final}$ by

$$\eta_{IQE} = \frac{\tau_{PL,final} - \tau_{PL,initial}}{\tau_{PL,final}}; \tag{48}$$

$$\frac{1}{\tau_r} = \frac{1}{2}\left(\frac{1}{\tau_{PL,initial}} - \frac{1}{\tau_{PL,final}}\right). \tag{49}$$

Therefore, one can find the IQE, the radiative recombination carrier lifetime (τ_r), and the nonradiative recombination carrier lifetime (τ_{nr}) simultaneously by a single measurement of the TRPL response at room temperature. Furthermore, one can expect intuitively that the sample with a relatively short $\tau_{PL,initial}$ and a long $\tau_{PL,final}$ can be regarded as a good sample according to Equation (48). Figure 3 summarizes the theory described thus far. The following is an experimental example of the TRPL analysis.

The measured TRPL responses are examined for three InGaN-based LED samples with different QW structures grown on c-plane sapphire substrates by the metal-organic chemical vapour deposition (MOCVD). Measurement setup consists of a picosecond light pulser and a streak scope. The wavelength of the pump light source is 405 nm in order to avoid excitation other than in QWs. All measurements are performed at room temperature. Their peak wavelengths are 460 nm for both sample 1 and sample 2, and 480 nm for sample 3. Normalized TRPL responses measured for these samples are shown in Figure 4. As time progresses, sample 1 and sample 2 show very similar characteristics and have a relatively long lifetime compared to sample 3.

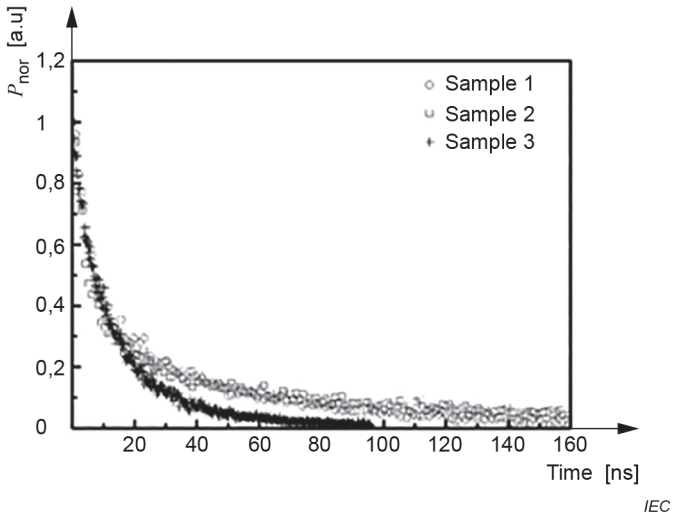

Figure 4 – Temporal responses of the TRPL for three samples

For analysis, the measured data is fitted by the least-mean-square method, with a combination of three-exponential functions to minimize the fitting error, and subsequently drawn on a logarithm scale in Figure 5. The fitted result of sample 1 in Figure 5 a) shows a short time range at the initial stage, and a relatively long time range where the curve can be fitted with a single exponential function. $\tau_{PL,initial}$ and $\tau_{PL,final}$ represent the lifetimes at the initial and final stages, respectively. While deducing the lifetimes, $\tau_{PL,initial}$ is estimated from $\ln P_{nor}(t) > -0{,}3$, whereas $\ln P_{nor}(t) < -3{,}5$ is used for $\tau_{PL,final}$. From the aforementioned time range, the measured $\tau_{PL,initial}$ and $\tau_{PL,final}$ are approximately 13,6 ns and 55,6 ns from the slope of $\ln P_{nor}(t)$ curve, respectively. Therefore, the IQE, τ_r, and τ_{nr} for sample 1 are found to be approximately 75,6 %, 35,9 ns, and 111 ns. The fitted results for samples 2 and 3 in Figure 5 b), the slope of the TRPL response at the final stage is shown as a straight line for each sample. From the figure, it may be intuitively predicted that the QW quality of sample 2 is much better than that of sample 3 because they show very similar initial slopes, whereas the slope of the final stage is much smaller for sample 3, which represents τ_{nr}. Estimated IQE values for samples 1, 2, and 3 are approximately 75,6 %, 78,4 %, and 32,6 %, respectively. Also, the lifetimes τ_{nr} are found to be approximately 111 ns, 96,6 ns, and 34,0 ns for samples 1, 2, and 3, respectively, whereas the lifetimes τ_r are approximately 35,9 ns, 26,6 ns, and 74,3 ns for the same samples. From the obtained results, it can be concluded that they show the same tendency as the intuitive prediction discussed above.

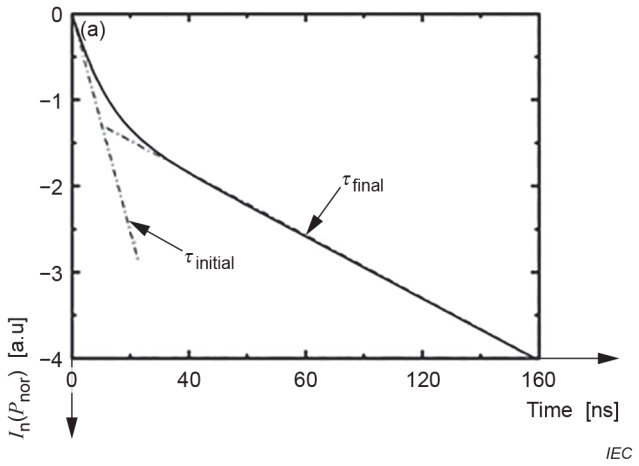

a) Fitted result of sample 1 and their lifetimes, $\tau_{initial}$ and τ_{final}

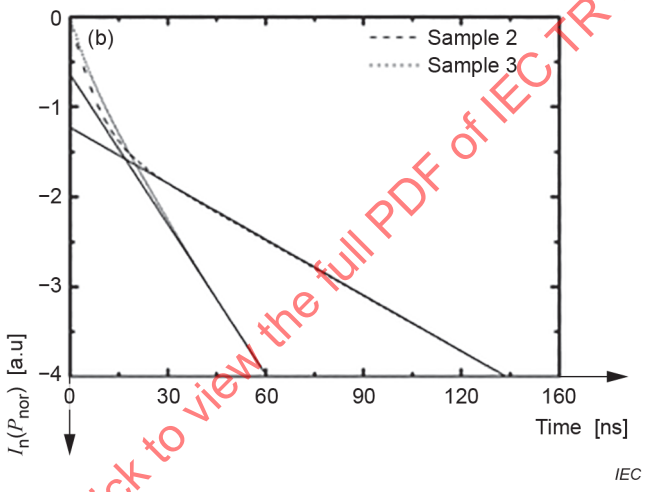

b) Fitted results of samples 2 and 3 with their final decay slopes drawn in straight lines

Figure 5 – Fitted results of the measured TRPL response

So far, the SRH recombination has only been considered as a dominant nonradiative recombination process. However, as the number of carriers increases, the nonradiative recombination due to the Auger recombination or carrier overflow is expected to become very large. Therefore, it should be noted that the analytical model presented here is applicable to a situation where a relatively low density of carriers exist in the active layers at room temperature.

In summary, a simple theory of carrier dynamics from the TRPL measurement at room temperature has been presented to obtain the carrier lifetimes and the IQEs of LEDs. The implications of the measured TRPL response curves have been discussed rigorously by solving the carrier rate equation in active QW layers. It has been shown that the radiative and nonradiative recombination processes compete with each other at the initial stage in the TRPL and is gradually dominated by the nonradiative recombination at the final stage. Furthermore, it has been found that the measured TRPL lifetimes differ from the carrier lifetimes by a factor of 2. In addition, the IQE has also been obtained from the room-temperature TRPL response without performing low-temperature measurements.

5.6 Time-resolved electroluminescence (TREL)

The TREL is reported for estimating the IQE based on data of EL decay times measured as a function of current in the pulse injection [79],[80]. With the Auger nonradiative recombination

$n(t)$ in the active layer

can be written as

$$\frac{dn}{dt} = \eta_{IE}\frac{I}{qV_{active}} - \frac{n}{\tau_s} = \eta_{IE}\frac{I}{qV_{active}} - \left(An + Bn^2\right), \tag{50}$$

$$\frac{1}{\tau_s} = \frac{1}{\tau_{s(nr)}} + \frac{1}{\tau_{s(r)}} = A + Bn, \tag{51}$$

where n, I, q, V_{active}, and η_{IE} are the carrier density, the forward current, the elementary charge, the active volume, and the IE into the active volume, respectively. A and B are coefficients of the SRH nonradiative recombination and the bimolecular radiative recombination, respectively. τ_s, $\tau_{s(nr)}$, and $\tau_{s(r)}$ are total, nonradiative, and radiative carrier lifetimes in the steady state, respectively. It should be noted that carrier lifetimes in the steady state are different from those in dynamic states.

Consider that the forward current is step-likely modulated from $I_o + \Delta I_o$ to I_o at $t = 0$ as shown in Figure 6. Equation (50) can be rewritten with the time evolution as

$$\frac{d\left(n_o + \Delta n\right)}{dt} = \eta_{IE}\frac{I_o}{qV_{active}} - A\left(n_o + \Delta n\right) + B\left(n_o + \Delta n\right)^2 \text{ with } \Delta n(t = 0^+) = \Delta n_o \text{ for } t \geq 0, \tag{52}$$

$$0 = \eta_{IE}\frac{I_o + \Delta I_o}{qV_{active}} - \left[A\left(n_o + \Delta n_o\right) + B\left(n_o + \Delta n_o\right)^2\right] \text{ for } t < 0, \tag{53}$$

$$0 = \eta_{IE}\frac{I_o}{qV_{active}} - \left(An_o + Bn_o^2\right) \text{ as } t \to \infty, \tag{54}$$

$$\frac{d\Delta n}{dt} = -\left[A\Delta n + 2Bn_o\Delta n + B\left(\Delta n\right)^2\right] \text{ with } \Delta n(t = 0^+) = \Delta n_o,\ \Delta n(t = \infty) = 0 \text{ for } t \geq 0 \tag{55}$$

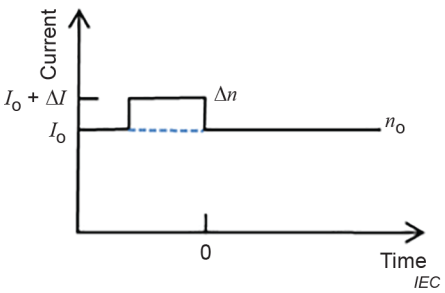

Figure 6 – Schematic diagram of the pulse current injection

The steady-state carrier density (n_o) at a bias current I_o and a variation of carrier density (Δn_o) resulting from a small current pulse (ΔI_o) are obtained from Equations (53) and (54) as follows:

$$n_{\mathrm{o}} = \frac{1}{2B}\left\{-A + \sqrt{A^2 + 4B\left(\eta_{\mathrm{IE}} \frac{I_{\mathrm{o}}}{qV_{\mathrm{active}}}\right)}\right\}, \tag{56}$$

$$n_{\mathrm{o}} + \Delta n_{\mathrm{o}} = \frac{1}{2B}\left\{-A + \sqrt{A^2 + 4B\left(\eta_{\mathrm{IE}} \frac{I_{\mathrm{o}} + \Delta I_{\mathrm{o}}}{qV_{\mathrm{active}}}\right)}\right\}, \tag{57}$$

$$\begin{aligned}\Delta n_{\mathrm{o}} &= \left(n_{\mathrm{o}} + \Delta n_{\mathrm{o}}\right) - n_{\mathrm{o}} = \Delta n\left(t = 0\right) \\ &= \frac{1}{2B}\left\{\sqrt{A^2 + 4B\left(\eta_{\mathrm{IE}} \frac{I_{\mathrm{o}} + \Delta I_{\mathrm{o}}}{qV_{\mathrm{active}}}\right)} - \sqrt{A^2 + 4B\left(\eta_{\mathrm{IE}} \frac{I_{\mathrm{o}}}{qV_{\mathrm{active}}}\right)}\right\} \\ &= \frac{1}{2B\tau_{\mathrm{d}}}\left(-1 + \sqrt{1 + 4\left(\eta_{\mathrm{IE}} \Delta I_{\mathrm{o}} \Big/ qV_{\mathrm{active}}\right) B\tau_{\mathrm{d}}^2}\right),\end{aligned} \tag{58}$$

$$\frac{1}{\tau_{\mathrm{d}}} = A + 2Bn_{\mathrm{o}} = \sqrt{A^2 + 4B\left(\eta_{\mathrm{IE}} \frac{I_{\mathrm{o}}}{qV_{\mathrm{active}}}\right)}. \tag{59}$$

By linear fitting of the $1/\tau_{\mathrm{d}}^2$ versus I_{o}, the coefficients of A and B in Equation (59) can be determined with the known values of η_{IE} and V_{active}. Finally, the IQE (η_{IQE}) is obtained from

$$\eta_{\mathrm{RE}}\left(I_{\mathrm{o}}\right) = \frac{Bn_{\mathrm{o}}^2}{An_{\mathrm{o}} + Bn_{\mathrm{o}}^2} = \frac{1 - A\tau_{\mathrm{d}}\left(I_{\mathrm{o}}\right)}{1 + A\tau_{\mathrm{d}}\left(I_{\mathrm{o}}\right)} = \frac{1/\tau_{\mathrm{s(r)}}}{1/\tau_{\mathrm{s(r)}} + 1/\tau_{\mathrm{s(nr)}}} = \frac{1/\tau_{\mathrm{s(r)}}}{1/\tau_{\mathrm{s}}}, \tag{60}$$

$$\eta_{\mathrm{IQE}} = \eta_{\mathrm{IE}} \cdot \eta_{\mathrm{RE}} \cdot \tag{61}$$

By measuring the differential carrier lifetime τ_d as a function of bias current I_o, the IQE can be calculated from Equations (59), (60), and (61) if η_{IE} and V_{active} are known. In general, it is considered that the IE (η_{IE}) is not constant but varies with the bias current, i.e., $\eta_{\mathrm{IE}}(I_o)$, when the bias current becomes high. Thus, an assumption of $\eta_{IE} = 100\%$ may not be valid at such high current levels.

In order to find the differential carrier lifetime at an initial time of $t = 0^+$, i.e., $\tau_{\mathrm{d}}(t = 0^+)$, it is necessary to relate the experimentally measurable time-resolved EL signal, $P_{\mathrm{EL}}(t)$, to the theoretically analysed temporal decay of the carrier density, $n(t)$. Finally, the time-dependent PL decay signals, $P_{\mathrm{EL}}(t)$, and its normalized PL signal at $t = 0$, $P_{\mathrm{nor,EL}}(t)$, are obtained as

$$P_{\mathrm{EL}}(t) = P_{\mathrm{EL,o}} + \Delta P_{\mathrm{EL}}(t) = \eta_{\mathrm{det}}\eta_{\mathrm{LEE}}V_{\mathrm{active}}Bn^2(t) = \eta_{\mathrm{det}}\eta_{\mathrm{LEE}}V_{\mathrm{active}}B\left(n_{\mathrm{o}} + \Delta n(t)\right)^2, \tag{62}$$

$$\Delta P_{\mathrm{EL}}\left(t\right) = \eta_{\mathrm{det}}\eta_{\mathrm{LEE}}V_{\mathrm{active}}B\left(2n_o + \Delta n(t)\right)\Delta n(t), \tag{63}$$

$$\Delta P_{EL}(t=0) = \eta_{det}\eta_{LEE}V_{active}B(2n_o + \Delta n_o)\Delta n_o . \quad (64)$$

Then,

$$\Delta P_{nor,EL}(t) = \frac{\Delta P_{EL}(t)}{\Delta P_{EL}(0)} = \frac{(2n_o + \Delta n)\Delta n}{(2n_o + \Delta n_o)\Delta n_o}. \quad (65)$$

The initial slope of $\Delta P_{nor,EL}(t)$ at $t = 0$ is expressed by

$$\left.\frac{d\Delta P_{nor,EL}(t)}{dt}\right|_{t=0} = \frac{2(n_o + \Delta n)}{(2n_o + \Delta n_o)\Delta n_o}\left.\frac{d\Delta n(t)}{dt}\right|_{t=0} . \quad (66)$$

The time-dependent carrier density $\Delta n(t)$ is found by solving Equation (55) as

$$\Delta n(t) = \frac{1}{B\tau_d}\frac{1}{Ce^{t/\tau_d} - 1} , \quad (67)$$

where $C = \frac{1 + B\tau_d\Delta n_o}{B\tau_d\Delta n_o}$. $\tau_d(I_o)$ is the differential carrier lifetime at current I_o defined in Equation (59) and is different from the static carrier lifetime $\tau_s(I_o) = 1/(A + Bn_o)$ in Equation (51). By differentiating $\Delta n(t)$ in Equation (67) with respect to time,

$$\left.\frac{d\Delta n(t)}{dt}\right|_{t=0} = \left.\frac{1}{B\tau_d}\frac{-Ce^{t/\tau_d}/\tau_d}{(Ce^{t/\tau_d} - 1)^2}\right|_{t=0} = -\frac{1}{B\tau_d^2}\frac{C}{(C-1)^2} = -\frac{(1 + B\tau_d\Delta n_o)\Delta n_o}{\tau_d} . \quad (68)$$

Finally, Equation (66) can be theoretically rewritten as

$$\begin{aligned}\left.\frac{d\Delta P_{nor,EL}(t)}{dt}\right|_{t=0} &= \frac{2(n_o + \Delta n)}{(2n_o + \Delta n_o)\Delta n_o}\left.\frac{d\Delta n(t)}{dt}\right|_{t=0} = -\frac{2(n_o + \Delta n_o)}{(2n_o + \Delta n_o)\Delta n_o}\frac{(1 + B\tau_d\Delta n_o)\Delta n_o}{\tau_d} \\ &= -\frac{2(n_o + \Delta n_o)}{(2n_o + \Delta n_o)}\frac{(1 + B\tau_d\Delta n_o)}{\tau_d},\end{aligned} \quad (69)$$

where n_o, Δn_o, and τ_d are in Equations (56), (58), and (59), respectively. There are three unknown constants in Equation (59), namely, the recombination coefficients, A and B, and the IE, η_{IE}. η_{IE} is usually assumed as 100 % for all current ranges. But this assumption is reasonable only when the carrier recombination rate in the active layer is sufficiently high so that the carriers accumulated in the active layer does not overflow above the potential barrier.

Here, the IE of 100 % is assumed when the current injection is so low that the carrier overflow from the active layer to the outside is negligible. In Equation (69), since the term on the left-hand side, $dP_{nor,EL}(t)/dt|_{t=0}$, is the experimental value, all the values of A, B, and τ_d can be found if either A or B is known. An approximate solution to Equation (55) is derived by assuming $n_o >> \Delta n$ and $\eta_{IE} = 1$:

$$\frac{d\Delta n}{dt} \cong \eta_{IE}\frac{I_o}{qV_{active}} - \left(An_o + Bn_o^2\right) - \left(A+2Bn_o\right)\Delta n = -\left(A+2Bn_o\right)\Delta n = -\frac{\Delta n}{\tau_d} \quad \text{for } t \geq 0 \tag{70}$$

where n_o and τ_d are in Equations (56) and (59), respectively. Then $\Delta n(t)$ is obtained as

$$\Delta n(t) = \Delta n_o \exp\left(-\frac{t}{\tau_{d,o}}\right) , \tag{71}$$

where

$$\Delta n_o = \left(\eta_{IE}\frac{\Delta I_o}{qV_{active}}\right)\frac{1}{A+2Bn_o} = \left(\eta_{IE}\frac{\Delta I_o}{qV_{active}}\right)\tau_d .$$

The time-dependent PL decay signals and its normalized PL signal at $t = 0$ are obtained as

$$P_{EL}(t) = P_{EL,o} + \Delta P_{EL}(t) = \eta_{det}\eta_{LEE}V_{active}B\left(n_o + \Delta n(t)\right)^2 \approx \eta_{det}\eta_{LEE}V_{active}B\left(n_o^2 + 2n_o\Delta n(t)\right), \tag{72}$$

$$\Delta P_{EL}(t) = \left(2\eta_{det}\eta_{LEE}V_{active}Bn_o\right)\Delta n(t) = \left(2\eta_{det}\eta_{LEE}V_{active}Bn_o\right)\Delta n_o \exp\left(-\frac{t}{\tau_d}\right) , \tag{73}$$

$$\Delta P_{nor,EL}(t) = \frac{\Delta P_{EL}(t)}{\Delta P_{EL}(0)} = \exp\left(-\frac{t}{\tau_d}\right). \tag{74}$$

The initial slope of $\Delta P_{nor,EL}(t)$ at $t = 0$ is expressed by

$$-\left.\frac{d\Delta P_{nor,EL}(t)}{dt}\right|_{t=0} = \left.\frac{1}{\tau_d}\exp\left(-\frac{t}{\tau_d}\right)\right|_{t=0} = \frac{1}{\tau_d} . \tag{75}$$

As a result, the time-dependent PL decay signal can be expressed by single exponential function with the decay time of $\tau_d(I_o)$ as a first approximation. Then, the coefficients of A and B in Equation (59) are known by the linear fitting of $1/\tau_d^2$ versus I_o and the IQE is finally obtained by Equation (60). As described previously, it is necessary to solve Equation (69) for a more accurate value of the IQE. One of the good options for this is to assume that a ratio of the recombination coefficients A and B obtained from Equation (69) is constant and taken as $A/B = k_{AB}$ and find k_{AB} by solving Equation (73) with $\eta_{IE} = 100\ \%$. Then, all the values of A, B, τ_d, and η_{IQE} are known. It should be noted that this analysis can be applied only to the case of $\eta_{IE} = 100\ \%$. Therefore, it is necessary to develop the TREL method that can include the effect of the IE change.

Here, an example of the TREL in reference [79] is shown. In this study, the time decays of the EL were measured on the pulse current injection with the bias voltage. The emission peak wavelength of the LED was 460 nm. With the amplitude of the pulse current set as constant, the bias current I_o J_o Figure 8. As a first approximation, the time decay of the EL in the pulse injection is approximated as a single exponential shape in Equation (74) and the current IE of 100 %. Then, the coefficients of A

and B in Equation (59) are found from the linear fitting of $1/\tau_d^2$ versus J_o and the IQE is finally obtained by Equation (60) as shown in Figure 7 and Figure 8, respectively.

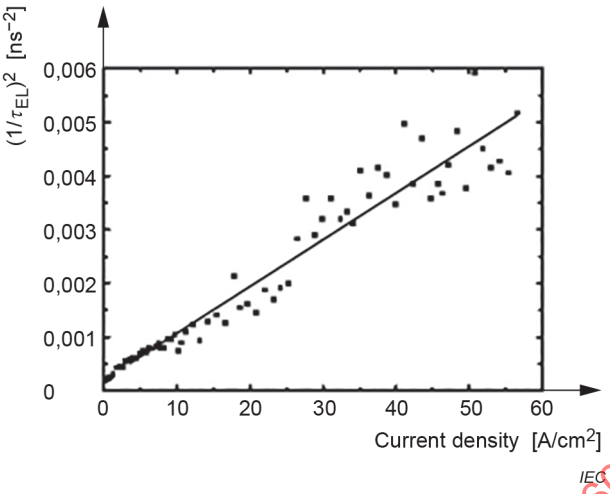

The solid line is a fit by Equation (59).

Figure 7 – Square of $1/\tau_{EL}$ as a function of current density for a bias voltage

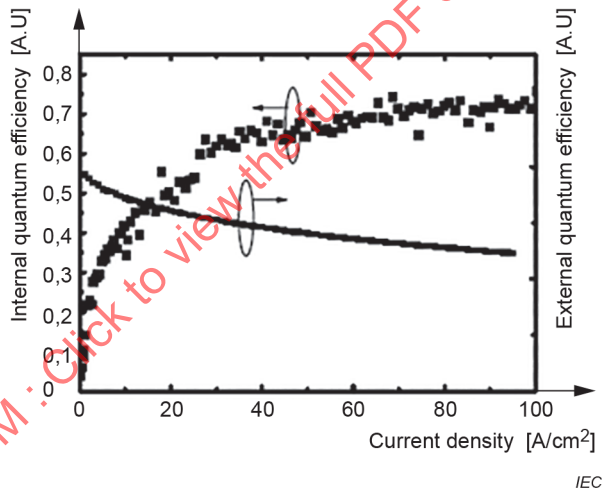

Figure 8 – Estimated IQE (left axis) and measured EQE (right axis) versus current density

5.7 Constant ABC model

The simplest and the most popular method of the IQE measurement satisfying all the conditions of (i)-(iv) mentioned in 4.4 is the constant ABC model [81]-[104]. The model is based on the carrier rate equation for the LED. Assumptions behind the model are as follows:

a) All carriers are injected into the active layers and recombine there. Thus, the IE is implicitly assumed as 100 % with a well-defined active volume V_{active}. In this case, the IQE becomes identical to the RE.

b) Nonequilibrium concentrations of electrons and holes in the active layers are nearly equal to each other.

c) Three recombination processes, i.e., the nonradiative SRH, radiative band-to-band, and nonradiative Auger recombinations, are considered and their recombination rates are

expressed with the recombination coefficients A, B, and C, respectively, and carrier concentration n. Note that A, B, and C coefficients are considered as certain *constants*.

d) The LEE is independent of the injection current. Thus, the IQE has the same shape as the EQE as a function of current.

With the electron and hole concentrations in the active QW region nearly equal to each other, the carrier rate equation is written as

$$\frac{dn}{dt} = G_{\text{inj}} - R = \eta_{\text{IE}} G - R = \eta_{\text{IE}} \frac{I}{qV_{\text{active}}} - \left(An + Bn^2 + Cn^3\right), \tag{76}$$

where n, η_{IE}, I, q, and V_{active} are the carrier density in the active layer, the IE, the injected current, the elementary charge, and the active volume, respectively. For the steady state where $dn/dt = 0$, the carrier injection rate is equal to the recombination rate, i.e., $G_{\text{inj}} = \eta_{\text{IE}} G = R$. Then,

$$I = \frac{qV_{\text{active}}}{\eta_{\text{IE}}}\left(An + Bn^2 + Cn^3\right);\ P_{\text{EL}} = \eta_{\text{c}} h\bar{\nu} V_{\text{active}}\left(Bn^2\right) \text{ and} \tag{77}$$

$$\eta_{\text{IQE}} = \eta_{\text{IE}} \frac{Bn^2}{An + Bn^2 + Cn^3}, \tag{78}$$

where P_{EL}, $h\bar{\nu}$, and η_{c} are the measured EL power, the mean photon energy, and the light coupling efficiency between an LED and an optical detector, respectively. Knowing V_{active} and assuming η_{IE}, the electron density n and the IQE η_{IQE} can be calculated from Equations (77) and (78) with respect to current by using A, B, and C coefficients as fitting parameters to the experimental EQE curves. In this fitting process, the IE is 100 % and the carrier recombination coefficients A, B, C are certain constants and independent of one another. Generally, the A and B coefficients are found in the current region smaller than the EQE peak current. And the C coefficient is fitted in the current region greater than the EQE peak current.

Here, a few noticeable theoretical results behind the constant ABC model are discussed. First, the IQE or the EQE dependence on the injection current I is analytically expressed with two fitting parameters, the maximum IQE value, $\eta_{\text{IQE,max}}$, and the current at $\eta_{\text{IQE,max}}$, $I_{\text{IQE,max}}$, as follows [84]:

$$\bar{\eta}_{\text{EQE}} = 1 - \frac{(1 - \eta_{\text{IQE,max}})}{2\eta_{\text{IQE,max}}}\left(1 + \bar{\eta}_{\text{EQE}} \frac{I}{I_{\text{IQE,max}}}\right)\sqrt{\bar{\eta}_{\text{EQE}} \frac{I_{\text{IQE,max}}}{I}}; \tag{79}$$

$$\bar{\eta}_{\text{EQE}} = \frac{\Phi_{\text{e}}/I}{\Phi_{\text{e,max}}/I_{\text{IQE,max}}}, \tag{80}$$

where Φ_{e} and $\Phi_{\text{e,max}}$ are radiant powers measured at currents I and $I_{\text{IQE,max}}$, respectively. Note that Equation (79) has no explicit dependence on A, B, and C coefficients and is unambiguously determined only by $I_{\text{IQE,max}}$ and $\eta_{\text{IQE,max}}$ values where $\eta_{\text{IQE,max}}$ and $I_{\text{IQE,max}}$ satisfy the condition of $d\eta_{\text{IQE}}/dI = 0$. Since $I_{\text{IQE,max}}$ is easily found experimentally by using the EQE vs. current relation, $I_{\text{IQE,max}}$ is the only fitting parameter in Equation (79) in practice.

Second, $\eta_{\text{IQE,max}}$ and $I_{\text{IQE,max}}$ are explicitly expressed by using the carrier recombination coefficients A, B, and C as follows:

$$\eta_{\mathrm{IQE,max}} = \frac{B}{B + 2\sqrt{AC}};\ I_{\mathrm{IQE,max}} = \frac{kA}{C}(B + 2\sqrt{AC}), \tag{81}$$

where $k = qV_{\mathrm{active}}/\eta_{\mathrm{IE}}$. By assuming $\eta_{\mathrm{IE}} = 1$, k is determined directly from the active volume V_{active}. From Equation (80), the A, B, C coefficients are related to each other through $\eta_{\mathrm{IQE,max}}$ and $I_{\mathrm{IQE,max}}$ as follows:

$$B = \frac{4\eta_{\mathrm{IQE,max}}k}{I_{\mathrm{IQE,max}}(1-\eta_{\mathrm{IQE,max}})^2}A^2\ ;\ C = \frac{4k^2}{I_{\mathrm{IQE,max}}^2(1-\eta_{\mathrm{IQE,max}})^2}A^3. \tag{82}$$

Third, each recombination current can be calculated from $\eta_{IQE}(I)$ as follows:

$$\begin{aligned} I_{\mathrm{SRH}} &= \left(\frac{1-\eta_{\mathrm{IQE,max}}}{2}\sqrt{\frac{\eta_{\mathrm{IQE}}I_{\mathrm{IQE,max}}}{\eta_{\mathrm{IQE,max}}I}}\right)I = \eta_{\mathrm{SRH}}I, \\ I_{\mathrm{rad}} &= \eta_{\mathrm{IQE}}I, \\ I_{\mathrm{Auger}} &= \left(\frac{(1-\eta_{\mathrm{IQE,max}})}{2}\frac{\eta_{IQE}}{\eta_{\mathrm{IQE,max}}}\sqrt{\frac{\eta_{IQE}I}{\eta_{\mathrm{IQE,max}}I_{\mathrm{IQE,max}}}}\right)I = \eta_{\mathrm{Auger}}I. \end{aligned} \tag{83}$$

It is interesting to note that the SRH, radiative, and Auger recombination currents have no explicit dependence on the A, B, C coefficients and that they can be expressed as a function of current from the known quantities, $\eta_{\mathrm{IQE,max}}$, $I_{\mathrm{IQE,max}}$, η_{IQE}, and I. At sufficiently high current where $I >> I_{\mathrm{IQE,max}}$, I_{Auger} is much higher than I_{SRH} and the nonradiative current I_{nr} is considered dominated by the Auger recombination current I_{Auger}.

The next task is to determine the maximum IQE value, $\eta_{\mathrm{IQE,max}}$ in Equation (79). Here, two approaches are introduced. The first is to select $\eta_{\mathrm{IQE,max}}$ that gives the best fit between the experimental EQE and the simulated curves by Equation (79). The first fitting procedure is as follows: (i) Experimentally measure a relative EQE curve as a function of current I, normalize the experimental EQE curve by the peak EQE value, and find $I_{\mathrm{IQE,max}}$. (ii) Simulate curves of η_{IQE} versus I for different $\eta_{\mathrm{IQE,max}}$ satisfying Equation (79). (iii) Select $\eta_{\mathrm{IQE,max}}$ that gives the best fit between the experimental and simulated curves from the step (i) and the step (ii), respectively. (iv) Calculate $k = qV_{\mathrm{active}}/\eta_{\mathrm{IE}}$ by assuming η_{IE} of unity and V_{active}. Finally, estimate A, B, and C coefficients from Equation (82) by assuming one of them, for example A. At last, calculate each recombination current in Equation (83).

Now the theoretical analysis of the IQE is compared with experimental efficiency curves. A commercial InGaN-based blue LED sample is used for the measurement of the output power as a function of current at room temperature. The peak wavelength of the emission spectrum is 460 nm. $I_{\mathrm{IQE,max}}$

Figure 9 and Figure 10, respectively. The theoretical IQE curves obtained by solving Equation (79) for different $\eta_{\mathrm{IQE,max}}$ are overlaid on the measured result of the EQE curve versus current. For this sample, a quite good agreement is observed up to 100 mA when $\eta_{\mathrm{IQE,max}}$ is 79%. Using $\eta_{\mathrm{IQE,max}}$, $I_{\mathrm{IQE,max}}$, and k of the LED sample, the relation between A and C coefficients can be found from Equation (82). Figure 11 shows the nonradiative carrier lifetime (τ_{SRH}) that is the inverse of the A coefficient as a function of the C coefficient. Recently reported A coefficient values of InGaN LEDs are between 0,5 × 10^7 s^{-1} and 2 × 10^8 s^{-1}, which correspond to τ_{SRH} of 5 ns − 100 ns. In Figure 11,

however, when τ_{SRH} lies between 5 ns to 200 ns, the corresponding range of the C coefficient is around 10^{-28} cm^6/s – 10^{-24} cm^6/s. To date, there are no theories explaining such large C coefficients. Thus, it is plausible that a carrier loss process with the n^3-dependence, obvious in the InGaN-based QW LEDs, may not represent the Auger process.

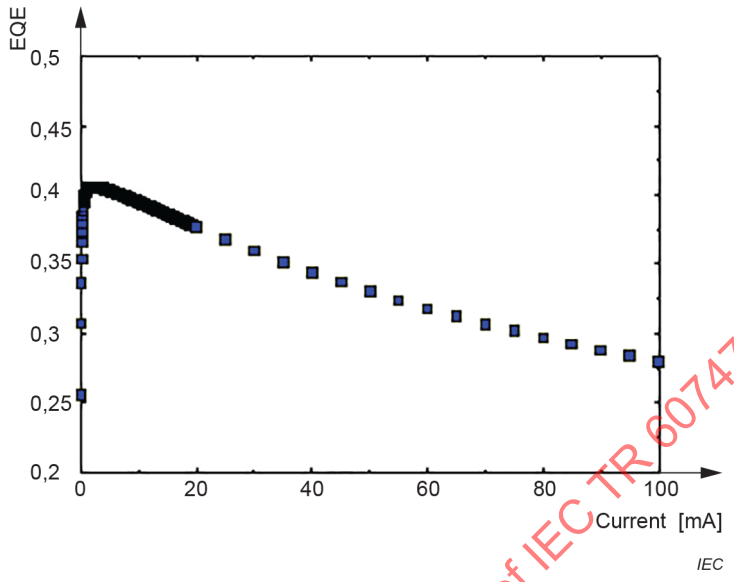

Figure 9 – Experimental EQE curve of a blue LED

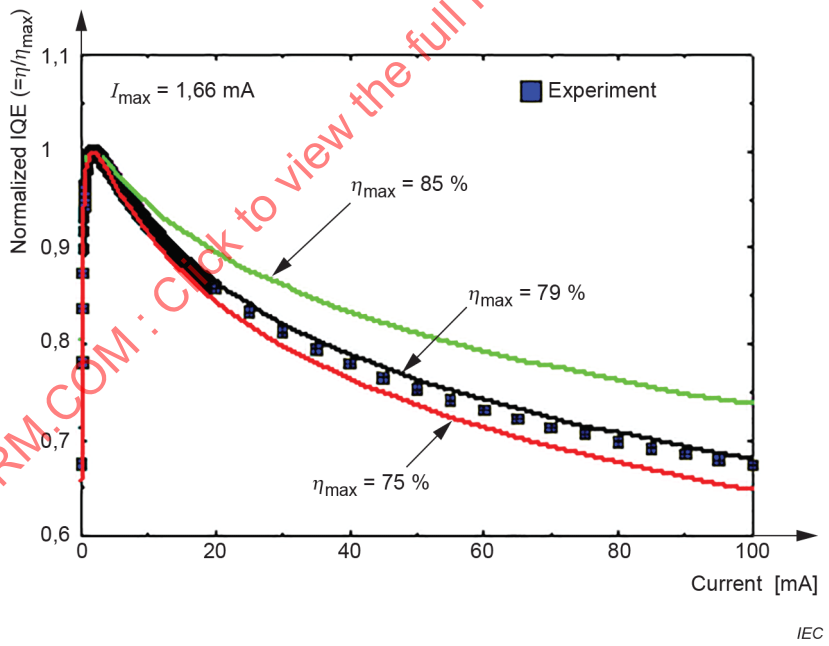

Figure 10 – Normalized EQE curves (solid lines) and experimental data (rectangular symbols) for different IQE peak values as a parameter for a blue LED emitting at 460 nm

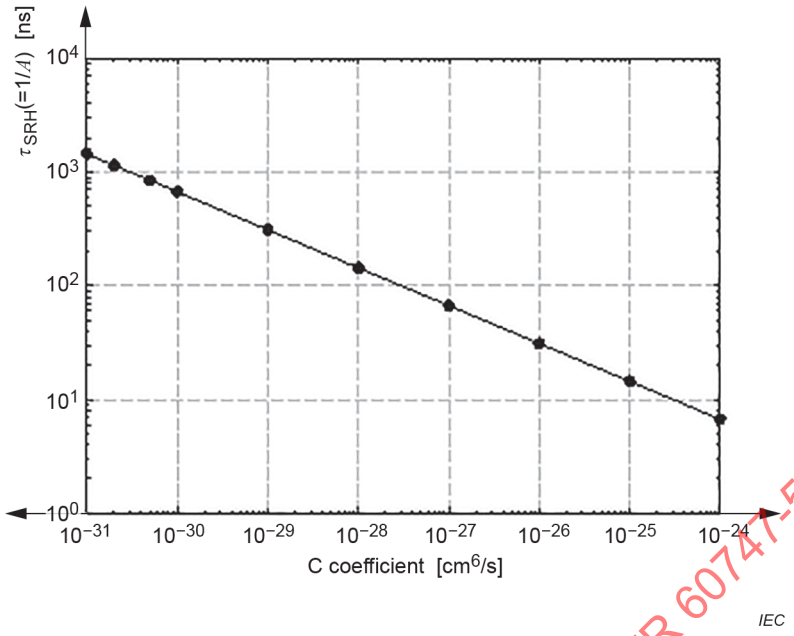

Figure 11 – SRH nonradiative carrier lifetime $\tau_{SRH}(=1/A)$ as a function of the C coefficient calculated from Equation (82)

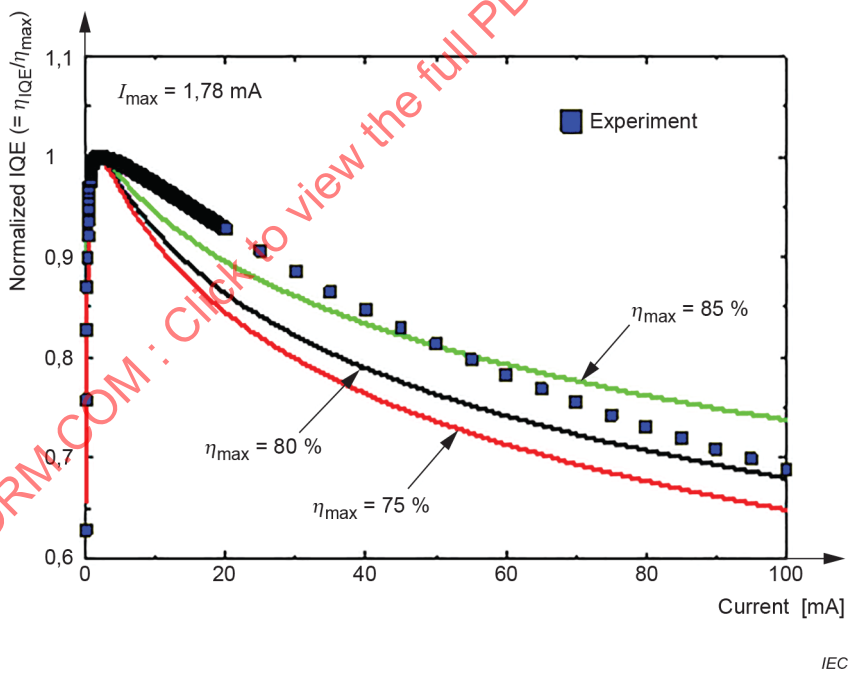

Figure 12 – Experimental EQE curve of a blue LED

Figure 12 shows another example of the normalized EQE curves (solid lines) for different IQE peak values as a parameter and an experimental data (rectangular symbols) for a 460-nm InGaN LED. In this sample, no $\eta_{IQE,max}$ value giving a good fit between the experimental data and the theoretical prediction can be found. This result implies that there would be a different nonradiative recombination mechanism at high injection current that cannot be described by n^3-dependence.

The second approach of finding $\eta_{IQE,max}$ is similar to the first: Equation (79) is rewritten as

$$\frac{1}{\bar{\eta}_{\mathrm{EQE}}} = \eta_{\mathrm{IQE,max}} + \frac{\left(\bar{\Phi}_{\mathrm{e}}^{1/2} + \bar{\Phi}_{\mathrm{e}}^{-1/2}\right)}{Q+2},\ \eta_{\mathrm{IQE,max}} = \frac{Q}{Q+2} \tag{84}$$

where $\bar{\Phi}_{\mathrm{e}} = \Phi_{\mathrm{e}} / \Phi_{\mathrm{e,max}}$ is the radiant power normalized by the peak EQE value. The factor $Q = B/\sqrt{AC}$ is a dimensionless invariant parameter and simply called the Q-factor. $\bar{\eta}_{\mathrm{EQE}}$ and Φ_{e} are experimental values of the EQE and the radiant power normalized by respective peak values. Plotting $1/\bar{\eta}_{\mathrm{EQE}}$ versus $\bar{\Phi}_e^{1/2} + \bar{\Phi}_e^{-1/2}$, approximating the plot by a linear function, and finding the intercept point of the line with the vertical axis and the slope, one can get the maximum IQE, $\eta_{\mathrm{IQE,max}}$, and the Q-factor [85]-[87].

However, the theoretical IQE, η_{IQE}, written as Equations (80) or (84) often deviates from the experimental IQE curve, $\eta_{\mathrm{IQE(e)}}$, which is defined as

$$\eta_{\mathrm{IQE(e)}} = \eta_{\mathrm{IQE,max}} \frac{\Phi_{\mathrm{e}} / I}{\Phi_{\mathrm{e,max}} / I_{\mathrm{IQE,max}}}, \tag{85}$$

where $\eta_{\mathrm{IQE,max}}$ is known from the fit of Equations (80) or (84) and the other parameters are experimentally measurable. It is thought that the difference of the experimental IQE, $\eta_{\mathrm{IQE(e)}}$, in Equation (85) and the theoretical IQE, η_{IQE}, satisfying Equations (80) or (84) results from an additional nonradiative recombination current, I_{leakage}, for the very high current range. By using Equation (76), I_{leakage} is calculated as

$$I_{\mathrm{leakge}} = I - \left(\eta_{\mathrm{SRH}} + \eta_{\mathrm{IQE}} + \eta_{\mathrm{Auger}}\right) I \tag{86}$$

The accuracy of the constant ABC model largely depends on the finding an exact value of $\eta_{IQE,\mathrm{max}}$ so that a best fitting is usually taken around the EQE peak or $I_{\mathrm{IQE,max}}$. However, one can often see that the data deviations from the ABC model predictions occur either at lower or higher currents from $I_{\mathrm{IQE,max}}$. The mechanisms tentatively responsible for low- and high-current deviations from the ABC model predictions are introduced in detail in References [98],[99].

Apart from experimental discrepancies, the ABC model has a few theoretical limitations to be a reliable IQE measurement method. It should be remembered that this analysis is extremely dependent on many assumptions that are unverified in real-world devices. Some neglected complications can significantly alter the shape of the EQE curve and consequently the parameter determination. The most suspicious assumptions are the following:

– A, B, and C coefficients are not really constants but dependent on carrier concentration n and
– the IE, η_{IE}, is not 100 % but a function of current.

Therefore, it is necessary to overcome theoretically and experimentally these technical hurdles arising from the constant ABC model for a consistent and reliable measurement of the IQE value as a function of current.

In summary, a very simple fitting method based on the constant ABC model in the carrier rate equation has been introduced. The method utilizes just two parameters of current at the IQE peak and the IQE peak value itself. It is possible to find the IQE and the carrier recombination currents simultaneously without any knowledge of A, B, and C recombination coefficients. In some InGaN LED, a good agreement has been obtained between the experimental and theoretical data with an Auger coefficient a few order of magnitude higher than the actually found. In another sample, the experimental data could not be well fitted with the theory. These experimental results imply that the constant ABC model is not suitable to be a standard IQE measurement method for InGaN LEDs. .

5.8 Constant AB model

Two types of carrier losses related to the IE have been known: (i) nonradiative recombination through defects in the bulk active layer and at all the boundaries of the active layers (interfaces and surfaces) and (ii) leakage out of the active region, i.e., carrier overflow. Usually, the two losses become important at low current levels far below the EQE peak and at high current levels around the EQE peak, respectively. In order to estimate the IQE exactly, each carrier loss needs to be identified quantitatively or at least relatively. However, separation of the carrier losses into these two types is usually very difficult [89],[105]-[107].

The restriction of the universal usage of the constant ABC model comes from the fact that the dominant nonradiative recombination process considered in the model at high current levels includes only the Auger recombination without identifying the influence of carrier overflow, i.e., the IE of 100 % with a well-defined active volume [80],[89]. Unfortunately, a method of experimentally discriminating between the Auger recombination and the carrier overflow is still controversial [83],[97],[100].

The constant AB model has been developed in order to eliminate such an unclear problem of the IE at high current levels involved in the constant ABC model [105]–[117]. The constant AB model is applied at low current levels around the onset of spontaneous emission in which the carrier loss of type (i) mentioned above becomes much more important than the carrier loss of type (ii). The crucial point is that all the losses of type (i) are thought to be directly proportional to the carrier concentration n in this regime. This implies that all these losses can be lumped together in a single overall proportionality constant, or in a single effective nonradiative carrier lifetime τ_{nr}, which is independent of n. A simple theory shows that this approximation is reasonable when all the carrier recombination losses of type (i) have constant "saturated" recombination velocities with a well-defined active volume. In this AB model, only an effective nonradiative recombination with a constant recombination coefficient A and the radiative recombination with a constant coefficient B are accounted for, assuming an IE of 100 % at low currents.

Therefore, methods based on the simpler AB model have been investigated to fit a low-current range far below the maximum EQE without considering the high-current region [105]-[117]. In these conventional constant AB models, the EQEs are fitted over a current range below a certain small current by assuming IE = 100 % with a constant LEE. The IQEs of some AlGaInP-based red LEDs could be successfully obtained by using the conventional constant AB models [109],[112]. However, many realistic LEDs usually show a certain amount of leakage currents of different nature in the low-current region. The surface current and the defect-related tunnelling current are also considered as possible leakage currents at low-current levels below the current at the maximum EQE. Thus, the EQE curves cannot be described by the conventional simple AB models with IE = 100 % over a wide current range.

The fitting procedure from the experimental EQE curve as a function of current has been reported originally in Reference [105] and recently in Reference [112]. The IQE of an LED can be estimated by

$$\eta_{\mathrm{IQE}} = \frac{\Phi_{\mathrm{e},12}^{1/2}}{\Phi_{0,5}^{1/2} + \Phi_{\mathrm{e},12}^{1/2}}, \tag{87}$$

where

$$\sqrt{\Phi_{0,5}} = \frac{\eta_{\mathrm{EQE},2} - \eta_{\mathrm{EQE},1}}{\eta_{\mathrm{EQE},1}/\sqrt{\Phi_{\mathrm{e},1}} - \eta_{\mathrm{EQE},2}/\sqrt{\Phi_{\mathrm{e},2}}};\ \Phi_{\mathrm{e},12} = \frac{\Phi_{\mathrm{e},1} + \Phi_{\mathrm{e},2}}{2} \tag{88}$$

In Equations (87) and (88), $\Phi_{\mathrm{e}} = \eta_{\mathrm{LEE}} \bar{h\nu} V_{\mathrm{active}} B n^2$ is the radiant power of the LED with the active volume V_{active} and nonequilibrium electron/hole concentration n. $\Phi_{0,5} = \eta_{\mathrm{LEE}} \bar{h\nu} V_{\mathrm{active}} A^2 B^{-1}$ is the radiant power corresponding to an IQE of 50 %. $\eta_{\mathrm{EQE,j}}$ and $\Phi_{\mathrm{e},j}$, where j = 1, 2, are the EQE and the radiant power of the LED measured at two different driving currents. Just for an IQE, it is not necessary for $\eta_{\mathrm{EQE,j}}$ to be absolute values. However, if the LEE is to be found, then absolute value of the EQE is required.

The constant AB model works well in some advanced LEDs where all the carrier losses of type (i) are so small that they are easily saturated at very small currents [109]. In reality, however, there are still many LED chips that have a large and unsaturated carrier loss of type (i). Therefore, it is necessary to check the assumptions IE = 100 % and the constancy of A and B recombination coefficients before applying the constant AB model [110].

6 Standard IQE measurement method I: TDEL

6.1 Temperature-dependent electroluminescence (TDEL) method

The separate and accurate measurement of the IQE as a function of injection current I at a certain temperature T has been a constant challenge since the advent of LEDs in early 1960s. For a generally acceptable measurement method of the IQE at a certain temperature, it is desirable to use experimentally measurable quantities such as the forward current and output radiant power without assuming any physical parameters, e.g., the chip size, epitaxial layer structures, carrier recombination rates, and complex refractive indices. Moreover, the IQE measurement methodology can be greatly simplified and improved in view of accuracy and reproducibility if the *relative* radiant power is used instead of the *absolute* radiant power. Two IQE measurement methods as a function of forward current are considered as the standard IQE measurement methods. The one is the temperature-dependent electroluminescence (TDEL) described in this section and the other is the room-temperature reference-point method (RTRM) based on the theoretical semiconductor carrier rate equation in Clause 7.

The TDEL method has been most popularly utilized with the longest history in the LED community and recognized as a standard method of IQE determination for LEDs [118]-[131]. This is partly due to the fact that it needs only a set of experimental data composed of the relative radiant power vs. forward current $(\Phi_{\mathrm{e}} - I)$ at various temperatures including cryogenic temperatures. The disadvantage of the TDEL method is that it requires an expensive and very stable cryogenic system with a long measurement time.

6.2 Temperature-dependent radiant power

Figure 13 a) shows the radiant powers of an LED at several temperatures from room temperature to low temperatures as a function of forward current. It is shown that the radiant power increases with decreasing temperature. This phenomenon is related to the deactivation of defects with decreasing temperature. Since the number of activated defects is a strong

function of temperature, the defects become deactivated as the temperature is lowered. It is called the defect "freeze-out". The number of activated defects can be expressed as

$$\text{number of defects} \propto \exp\left(-\frac{E_a}{k_B T}\right) \tag{89}$$

where E_a is the activation energy of defects and k_B is the Boltzmann constant. Since the defects are nonradiative recombination centres, the EL properties are strongly affected by temperature. With lowering temperature, the nonradiative recombination rate decreases, resulting in an increase of the radiant power.

Figure 13 b) depicts the relative EQE curves as a function of forward current measured in the wide range of temperature. Note the log scale for the x-axis. The relative EQE means the efficiency of the radiant power, i.e., a radiant power over a forward current. All the EQE curves exhibit similar shapes. However, the widths of the EQE curves gradually increase with decreasing temperature. It is noted that the maximum values are shifted to lower currents at the same time. The EQE peak also begins to form a plateau below a specific temperature.

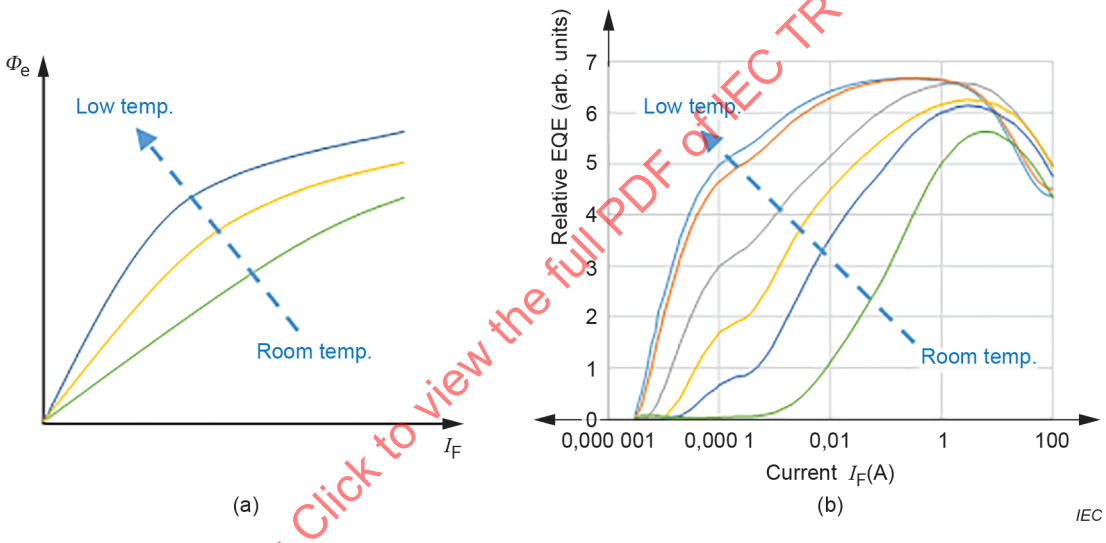

Figure 13 – Temperature characteristics of an LED

6.3 Evaluation of the IQE

Two important assumptions are introduced in the TDEL method. The first is that the LEE is constant, independent of forward current I and temperature T, so that the EQE should be linearly proportional to the IQE for any I and T. This assumption enables finding the IQE at any I and T only by comparing the EQE in question with the EQE at a so-called reference current and temperature, I_{ref} and T_{ref}, at which the IQE is exactly known as $\eta_{IQE,ref}$. In general, the reference point I_{ref} and T_{ref} is selected for $\eta_{IQE,ref} = 1$ such that both the IE and the RE are 100 % there. To find the reference point satisfying $\eta_{IE} = \eta_{RE} = 1$, the second assumption is used. At cryogenic temperatures, the nonradiative recombination centres in the active layer, which induce the SRH recombination, are "frozen" and become inactive. Moreover, the direct Auger recombination rate in conventional semiconductors decreases exponentially with decreasing temperature so that the contribution of the Auger recombination rate is also neglected at the reference point. By assuming that both the SRH and Auger recombination rates are negligibly small at cryogenic temperatures, the RE is considered as 100 % [43]-[45]. In general, the assumption of $\eta_{RE} = 1$ is experimentally confirmed by the fact that the peak EQEs at cryogenic temperatures do not increase further and maintain the maximum value with decreasing temperature.

With the RE of 100 %, the EQE is linearly proportional to the IE so that the peak of the EQE should correspond to the maximum IE. In this method, the IE is also taken as 100 % when it is experimentally confirmed that the peak value of the EQE does not vary with current in a limited range [123],[124]. As the reference point corresponding to an IQE of 100 % is decided this way, the IQEs at other operating conditions is determined by taking the ratio as shown below:

$$\eta_{\mathrm{IQE}}(I,T)=\frac{\eta_{\mathrm{EQE}}(I,T)}{\eta_{\mathrm{EQE}}(I_{\mathrm{ref}},T_{\mathrm{ref}})} \tag{90}$$

Note that η_{EQE} can be a relative EQE obtained from the relative radiant power since only the ratio is taken to obtain the IQE.

Some basic postulations are needed in order to determine the IQE of an LED by the TDEL method: (i) The LEE is assumed as constant for all operating conditions. (ii) The IQEs are assumed as 100 % for the limited condition of T_{LT} and I_{peak}, where the maximum values in relative EQEs are saturated. (iii) At the IQE of 100 %, both the IE and the RE are also assumed as 100 %, implying that all carriers are injected into the active layers and that they recombine only radiatively, because the IQE is a product of the IE and the RE. (iv) The LEE is assumed as the same for all temperatures and constant independent of the forward current.

In Figure 13 b), the IQE maximum is shifted towards lower forward currents with decreasing temperature. The peak values of the IQEs are eventually saturated and form a plateau. The lowest temperature that shows this behaviour is called T_{LT}. At T_{LT}, the maximum EQE values are considered corresponding to an IQE of 100 % (also IE and RE of 100 %). As the reference point corresponding to an IQE of 100 % is decided in this way, the IQEs at other operating conditions can be determined as shown in Equation (91):

$$\eta_{\mathrm{IQE}}(T,I_{\mathrm{F}})=\frac{\eta_{\mathrm{EQE}}(T,I_{\mathrm{F}})}{\eta_{\mathrm{EQE}}(T_{\mathrm{LT}},I_{\mathrm{peak}})}=\eta_{\mathrm{IE}}(T,I_{\mathrm{F}})\times\eta_{\mathrm{RE}}(T,I_{\mathrm{F}}), \tag{91}$$

where $\eta_{\mathrm{IQE}}(T,I_{\mathrm{F}})$, $\eta_{\mathrm{EQE}}(T,I_{\mathrm{F}})$, $\eta_{\mathrm{EQE}}(T_{\mathrm{LT}},I_{\mathrm{peak}})$, $\eta_{\mathrm{IE}}(T,I_{\mathrm{F}})$, and $\eta_{\mathrm{RE}}(T,I_{\mathrm{F}})$ represent the absolute IQE at T and I_{F}, the relative EQE at T and I_{F}, the relative EQE at the lowest cryogenic temperature T_{LT} and the peak current I_{peak} showing the maximum EQE, the IE at T and I_{F} and the RE at T and I_{F}, respectively.

Figure 14 is redrawn from Figure 13 b) after converting the relative EQE into the IQE as outlined above. The relative EQE curve is divided by the value of the maximum EQE, and then the maximum value of the converted curve is defined as an IQE of 100 % as expressed in Equation (91). Figure 14 represents the IQE of an LED at different operating temperatures plotted against the forward current.

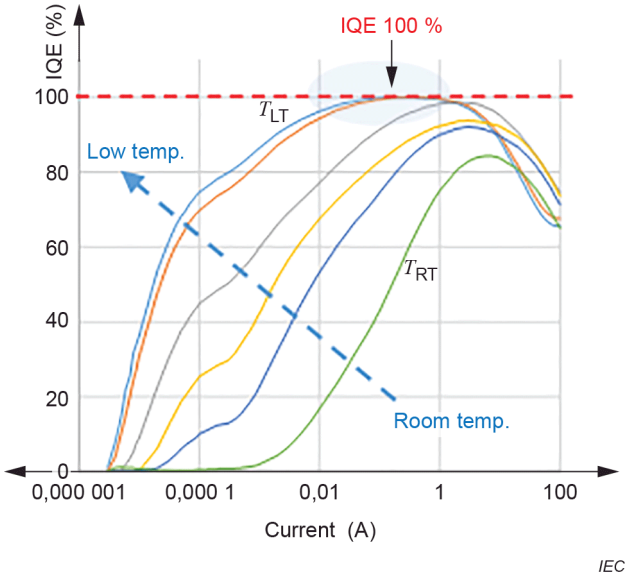

Figure 14 – IQEs as a function of current at various operating temperatures from room to cryogenic measured by the TDEL method

6.4 Validity of the TDEL: examples of blue LEDs

In the TDEL method, one should be careful whether the relative EQE curves at cryogenic temperatures can be applied to determine the IQE curve at room temperature. The limitation in applying the TDEL method is discussed. Figure 15 a) and (b) show different shapes of the relative EQE curves as a function of forward current for various temperatures for two blue LED samples. The samples are commercial LEDs from two different companies, both with lateral electrodes. The chip sizes and dominant wavelengths are 290 × 590 μm^2 and 458 nm for the sample shown in Figure 15(a) and 280 × 550 μm^2 and 447 nm for the one in Figure 15 b). Figure 15 a) shows that the relative EQE maximum does not increase further at temperatures below 50 K. In this case, the IE and RE (thus IQE) can be assumed to be 100 % and the IQE at operating conditions can be determined by Equation (91). However, some samples do not show such behaviours at cryogenic temperatures. In Figure 15 b), the relative EQE maximums keep varying with decreasing temperature: the maximum of the relative EQE curves occur at 100 K and then starts to decrease at temperatures lower than 100 K. In this case, the assumptions mentioned above are not satisfied: the TDEL method is not applicable to the LED samples showing this kind of behaviour. This kind of behaviour is caused by the carrier leakage still remaining via processes like tunnelling even with decreasing temperature, making the assumption that the maximum IE at the lowest cryogenic temperature is 100 % invalid [123]. Thus, it is very important to note that the IQE determination by the TDEL method is not always possible: one need to confirm whether the validity criterion with the relative EQE curves with temperature, as outlined above, is satisfied to apply the TDEL method to the LED sample under test.

This behaviour shown in Figure 15 b) is often observed with highly defective samples, but the physical reason for this is still controversial. Here, the following explanation is presented. Carrier leakage due to the tunnelling process is more dependent on the electric field than temperature. Thus, it is expected that the amount of leakage would not change significantly with temperature. In addition, the SRH nonradiative recombination rate monotonically increases with increasing temperature. Therefore, the increase of the EQE peak with increasing temperature as shown in Figure 15 b) is hardly understood only by the temperature dependence of the nonradiative recombination rate. But it is natural to think that the radiative recombination rate increases as the temperature increases at cryogenic temperatures. The radiative recombination rate is directly proportional to the distributions of electron-hole pairs that can recombine in real space as well as in energy (or momentum) space. The highly defective InGaN/GaN QW samples are thought to have quantum-dot- or quantum-disk-like active areas due to the random fluctuations of composition and stress field, resulting in a lower electronic density of states (DOS) compared to an ideal two-dimensional QW. A LED device having a small DOS exhibits

a rapid increase in the radiative recombination rate even at small currents at cryogenic temperatures, but easily saturate with increasing current levels. [118],[132]. Figure 15 b) is thought to show the EQE characteristics for these kinds of samples.

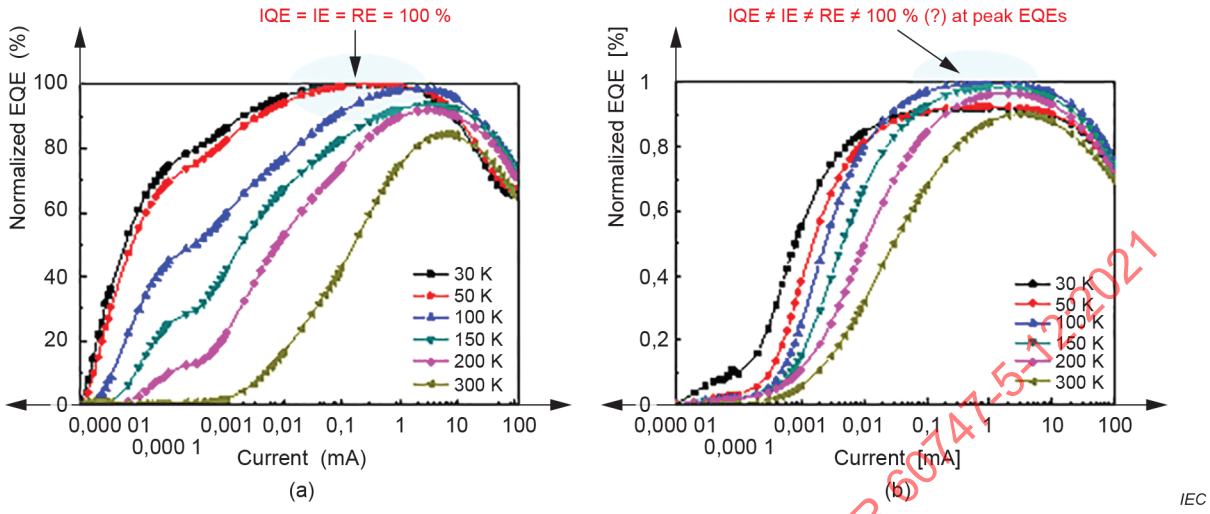

Figure 15 – Two different cases of normalized EQE curves as a function of current at various temperatures

6.5 Sequence of IQE determination by the TDEL

Figure 16 shows the sequence of the IQE determination by the TDEL method. Firstly, the radiant powers are measured as a function of forward current at various temperatures including the cryogenic temperature. Then the curves of radiant power versus forward current are converted to the relative EQE curves. Before proceeding further, it is very important to confirm whether the validity criterion is satisfied: if the peak EQE saturates with decreasing temperature, the TDEL method is applicable to this LED sample. Then, normalize the EQE curve by the maximum EQE value in the measurement and obtain the IQE curves at various temperatures. If the peak EQE does not saturate, one should stop the IQE measurement using the TDEL. The method is not applicable to this kind of LED sample.

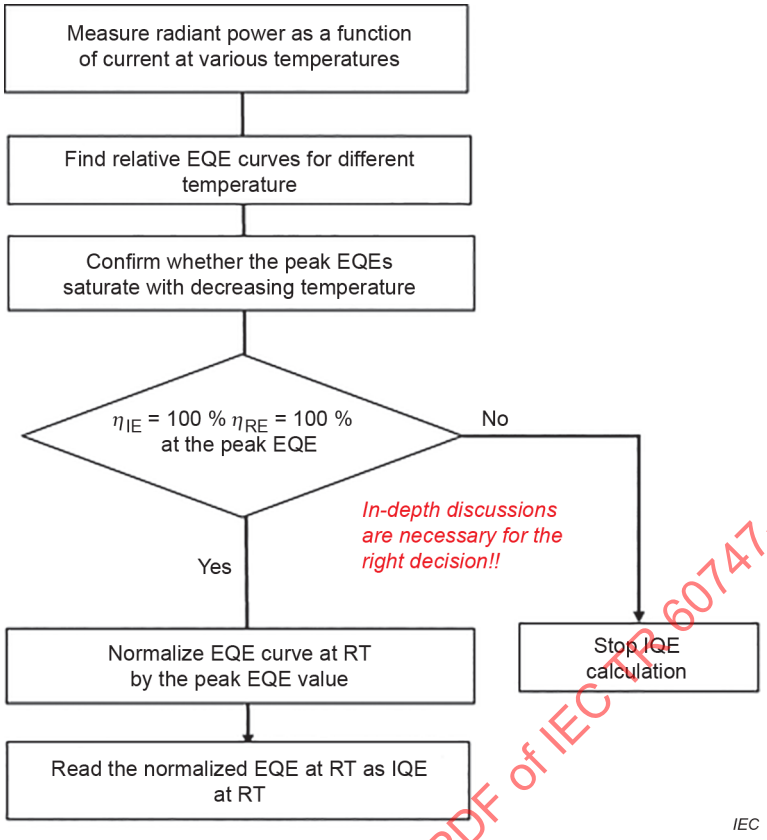

Figure 16 – Sequence of the IQE measurement by the TDEL method

6.6 Summary of the TDEL

The TDEL method has been described as a standard IQE measurement method with the discussions of basic postulations and validity criterion. Since the TDEL method does not require any values of material and structural parameters as well as the absolute radiant power, it has been widely utilized to measure the IQE of LEDs in the community. While there are disadvantages with the TDEL such as requiring an expensive and very stable cryogenic system during the long measurement time, the IQE measured by the TDEL can still serve as a useful reference value if the validity criterion is met.

7 Standard IQE measurement method II: RTRM

7.1 Room-temperature reference-point method (RTRM)

Although the TDEL is a generally accepted method of measuring the IQE as a function of current only from the experimental EQE curves measured at different temperatures ranging from room to cryogenic, it is very time- and labour-consuming. Lowering the temperature to cryogenic ones as low as approximately 20 K takes several hours using a helium-closed cycle system. Including preparation and actual measurements, the total testing would take a few hours. Moreover, one should be careful of the fundamental assumption used in the TDEL method that the LEE is independent of the temperature from the cryogenic to room temperatures. Sometimes, the LEE seems very dependent on the temperatures especially for narrow-bandgap semiconductors such as GaAs- or InP-based material systems. Thus, the needs for a method that can measure the IQE just at room temperatures arise.

Here, an IQE measurement method for an LED as a function of current at a fixed operating temperature is demonstrated without assuming IE = 100 % and the constancy of the recombination coefficients for a wide current range, different from the conventional AB(C) models. No material or structural parameters of an LED are used. The approach is called the room-temperature reference-point method (RTRM) [133], [134]. It utilizes a relative EQE curve

$\eta_{IQE,ref}$ is exactly known.

Unlike the TDEL, however, a reference point satisfying $\eta_{IE} = \eta_{RE} = 1$ cannot be sought because the experimental temperature is not cryogenic but a higher operating temperature. Thus, it is necessary to develop a unique strategy to overcome such a hurdle.

7.2 Recombination coefficients, A, B, and C in semiconductors

Before the semiconductor rate equation applied to the IQE measurement, the carrier recombination processes in the active layer are revisited [135]:

$$\begin{aligned} R(n,p) &= R_{SRH} + R_{spon} + R_{Auger} \\ &= \frac{(np - n_o p_o)}{\tau_p (n + n_1) + \tau_n (p + p_1)} + B(np - n_o p_o) + (C_n n + C_p p)(np - n_o p_o) \end{aligned} \quad (92)$$

Where n and p are electron and hole densities, respectively. τ_n and τ_p are the SRH recombination lifetimes for electrons and holes, respectively. B is the radiative recombination coefficient. The Auger coefficients C_n and C_p account for the two possible Auger processes, transferring the recombination energy to an electron in the conduction band and a hole in the valence band, respectively.

Usually, the active layers of modern LEDs are unintentionally doped. Thus, the equilibrium carrier density product $n_o p_o$ is much smaller than np even at low current injection levels. The defect parameters n_1 and p_1 are also often neglected. In the case that η_{IE} is almost unity, most of the carriers injected into an LED recombine inside the active layer and the charge neutrality condition is satisfied there. A nearly intrinsic active layer is considered such that $n \approx p >> n_o, p_o, n_1$, and p_1. For simplicity, the carrier capture times are set as constant, i.e., $\tau_n = \tau_p = (1/2)\tau_{SRH} = 1/A_{SRH}$. Then, the final result of the SRH recombination is asymptotically written as $R_{SRH} = A_{SRH} n$. In fact, this approximation is valid theoretically under low-level injection or small deviation from electrical equilibrium. Under high-level injection near the peak of η_{EQE}, however, it is more reasonable that A_{SRH} is dependent on the carrier density n, i.e., $A_{SRH}(n)$, rather than constant.

The radiative recombination rate R_{spon} is fundamentally determined by the Fermi golden rule, i.e., the $\vec{k}$-selection rule between electrons in the conduction band and holes in the valance band. It is typically approximated as $R_{spon} = Bnp$ for $np >> n_o p_o$ as written in Equation (92). The B coefficient is usually approximated as constant under low-level injection, but it monotonically decreases when the carrier density deviates from the Maxwell-Boltzmann distribution. Thus, the B coefficient is taken as a function of carrier density, i.e., $B(n)$ even for current levels less than the peak of η_{EQE}.

The Auger recombination rate R_{Auger} in Equation (92) is simplified as $R_{Auger} = Cn^3$ with $n = p$, $np >> n_o p_o$, and $C = C_n + C_p$. The Auger coefficient C takes into account all the possible Auger recombination processes such as the band-to-band, phonon-assisted, and defect-assisted Auger processes. In the band-to-band Auger process, C decreases exponentially with increasing bandgap energy and decreasing temperature, which arises from the conservation laws of energy and momentum among the four particle states. Consequently, the band-to-band Auger process is negligibly small in visible InGaN-based LEDs due to their wide bandgap energies. On the other hand, the phonon- or defect-assisted Auger process satisfies the

momentum conservation law through phonon or defect participation, respectively, making it a second-order Auger process. It is theoretically known that recombination coefficients C for the phonon- and defect-assisted Auger processes are similar but less sensitive to temperature and carrier density than that for the band-to-band Auger process.

Based on these discussions, many variations of the ABC model have been proposed in the literature [81]-[104]. The IE accounts for recombinations outside the active layer (carrier leakage). Most of the ABC models neglect the IE so that all the energized carriers are assumed to be injected and recombine only at the active layer. Moreover, their recombination coefficients A, B and C are assumed to be constant in the whole experimental current range. With such ABC models, the Auger process is only responsible for the efficiency droop at high current densities since the recombination rate Cn^3 is the only one that rises faster than the photon emission rate Bn^2 with increasing carrier density.

There have been many different reports on procedures of fitting experimental EQE curves using constant recombination coefficients A, B and C. In fact, various A, B and C parameter sets give identical IQE characteristics and a large variation in the extracted Auger parameter is possible if the carrier density in the active QW is not precisely known. The carrier density n is typically determined by carrier-lifetime measurements with the same assumption of $\eta_{\mathrm{IE}} = 1$. Some reports specially prepare a single QW LED in order to avoid the issue of nonuniform carrier distributions in multiple-quantum-well (MQW) regions. Nevertheless, the popular ABC model is not sufficient to obtain consistent values of A, B and C coefficients, especially the Auger coefficient C. Also, the curve fitting based on the ABC model often shows significant deviation from the measured efficiency. It is believed that these discrepancies mainly result from an approximation $\eta_{\mathrm{IE}} = 1$ for all current ranges. Therefore, it is necessary to confirm that IE can be approximated as unity before calculating A, B and C coefficients from the experimental EQE and the carrier density from the carrier lifetime curves.

7.3 Strategy of the IQE measurement just at an operating temperature

Figure 17 schematically compares the conventional ABC model with the improved AB model that the RTRM is based on. Following an approach similar to the TDEL method, the AB model also finds the reference current I_{ref} at which $\eta_{\mathrm{IQE,ref}}$ can be known exactly. Then, η_{IQE} at an arbitrary current I can be obtained from the relative ratio of $\eta_{\mathrm{EQE}}(I)/\eta_{\mathrm{EQE}}(I_{\mathrm{ref}})$. As expected, it is not possible to find $\eta_{\mathrm{IQE,ref}}$ satisfying $\eta_{\mathrm{IE}} = \eta_{\mathrm{RE}} = 1$ at room temperature. But there exists a current at which η_{IE} is most probably considered as 100 %. This current is the reference current I_{ref} in this method. However, η_{RE} at I_{ref} is less than 100 %.

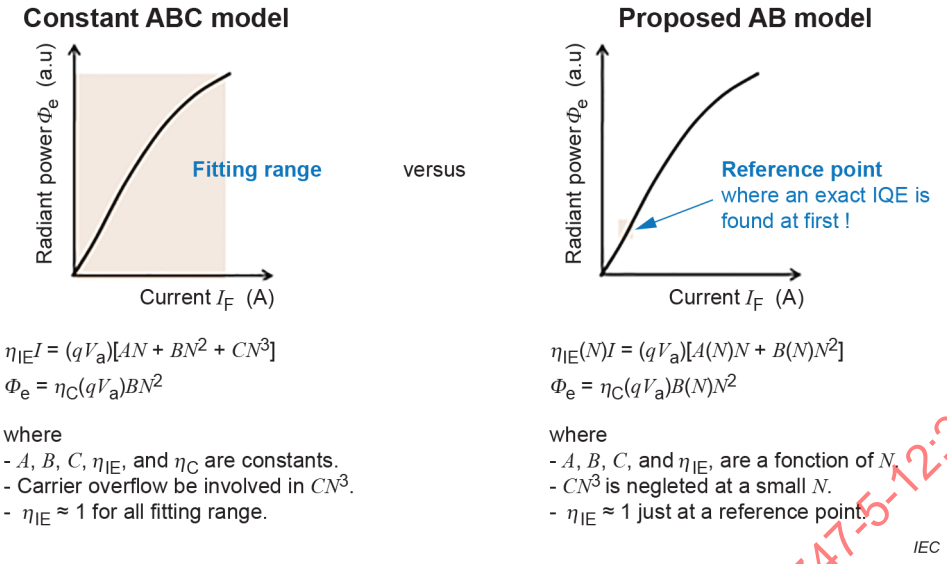

Figure 17 – Comparison between the conventional ABC model and the improved AB model

Figure 18 shows a conceptual illustration of the RTRM. Once the absolute $\eta_{IQE,ref}$ at I_{ref} is obtained from the experimental η_{EQE}, η_{IQE} at an arbitrary driving current I is obtained by $\eta_{IQE,ref}\,\eta_{EQE}(I)/\eta_{EQE}(I_{ref})$. Here, no material or structural parameters of an LED is required. The detailed explanation on how to find $\eta_{IQE,ref}$ is explained later with a blue LED sample.

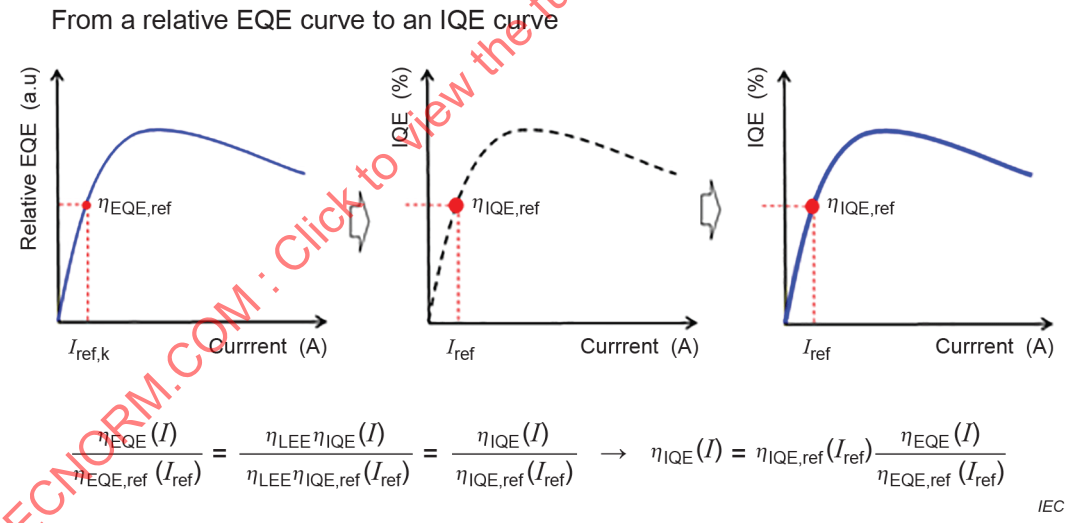

Figure 18 – Calculation procedure from a relative EQE curve to an IQE curve with the RTRM

7.4 Theoretical background of the RTRM

The RTRM is a method to solve the technical problems in the constant ABC and AB models [133]. This improved model includes the following elements: (a) the recombination coefficients A, B, and C are not constant but depends on the carrier density n; (b) the nonradiative Auger recombination is negligibly small at low currents far from the maximum EQE current, I_{max}. In this current range, the AB model instead of the ABC model is possible; (c) the IE is a function of current I or carrier density n so that there is a certain current, called the reference current I_{ref}, where the IE is maximized; (d) the LEE is assumed as constant so that an experimentally observed EQE curve is the same as the IQE curve. Thus, the IQE dependence on current can

be obtained once an IQE is exactly known at one point of the reference current I_{ref}. This approach is very similar to the TDEL method where operating conditions of current and cryogenic temperature are searched for the IQE to be assumed as 100 %; and (e) the IE at I_{ref} is considered as high as 100 % if any special attentions are not required.

In this improved AB model, the spontaneous radiant power detected by a photodetector Φ_e and the injection current I are formulated as follows:

$$\Phi_e(n) = \eta_c q V_{active} B(n) n^2, \tag{93}$$

$$\eta_{IE}(n) I = q V_{active} R(n) = q V_{active} \left[A(n) n + B(n) n^2 \right], \tag{94}$$

where η_c is the detector coupling efficiency, q is the elementary charge, and V_{active} is the active volume of the LED device. $A(n)$ and $B(n)$ are the SRH and radiative recombination coefficients, which are functions of carrier density n. As in typical rate equation analyses, the electron and hole densities are assumed to be approximately equal at the active region. The EQE is expressed as

$$\eta_{EQE}(n) = \eta_{LEE} \cdot \eta_{IE}(n) \cdot \eta_{RE}(n) = \eta_{LEE} \cdot \eta_{IE}(n) \cdot \frac{B(n) n^2}{A(n) n + B(n) n^2}. \tag{95}$$

Note in this AB model that any leakage other than the SRH recombination, such as the surface leakage and the defect-related tunnelling, contributes to making the IE less than unity.

Equations (93) and (94) are normalized by their corresponding values at the peak EQE in order to eliminate ambiguous constants of η_c and V_{active}. The carrier density, radiant power, and current at the peak EQE are denoted as n_p, $\Phi_e(n_p)$, and $I(n_p)$, respectively. Then, a very simple quadratic equation is obtained:

$$Y = a_1 X + a_2 X^2, \tag{96}$$

where $Y = I/I_p = I(n)/I(n_p)$ and $X = \sqrt{P_o(n)/P_o(n_p)}$. Both X and Y are experimentally measurable parameters. The a_1 and a_2 coefficients are

$$a_1(n) = \left[\frac{n_p \eta_{IE}(n_p) \sqrt{B(n_p)}}{A(n_p) n_p + B(n_p) n_p^2} \right] \frac{1}{\sqrt{B(n)}} \frac{A(n)}{\eta_{IE}(n)} = K_1(n_p) \frac{1}{\sqrt{B(n)}} \frac{A(n)}{\eta_{IE}(n)} \tag{97}$$

$$a_2(n) = \left[\frac{B(n_p) n_p^2 \eta_{IE}(n_p)}{A(n_p) n_p + B(n_p) n_p^2} \right] \frac{1}{\eta_{IE}(n)} = K_2(n_p) \frac{1}{\eta_{IE}(n)} \tag{98}$$

where $K_1(n_p)$ and $K_2(n_p)$ are constants, but $a_1(n)$ and $a_2(n)$ are functions of carrier density n. The radiative efficiency at a carrier density n is expressed as

$$\eta_{\mathrm{RE}} = \frac{a_2 X^2}{a_1 X + a_2 X^2}\,. \tag{99}$$

As in the following example, $a_1(n)$ and $a_2(n)$ vary very slowly compared to x and y. Thus, the functions $a_1(n)$ and $a_2(n)$ are obtained by solving two simultaneous equations from Equation (96) with two nearest experimental data $(X_{\mathrm{i}},\ Y_{\mathrm{i}})$ and $(X_{\mathrm{i+1}},\ Y_{\mathrm{i+1}})$. It should be noted from Equation (98) that $a_2(n)$ is inversely proportional only to $\eta_{\mathrm{IE}}(n)$. Thus, $\eta_{\mathrm{IE}}(n)$ would be the maximum when $a_2(n)$ is the minimum. It is reasonable in modern LEDs that there exists a current $I(n_{\mathrm{ref}})$ where $\eta_{\mathrm{IE}}(n_{\mathrm{ref}})$ is 100 % in a range of $I(n_{\mathrm{ref}}) < I(n_{\mathrm{p}})$. It should be noted that although the carrier density n is used in the formalism, it is purely symbolic: any knowledge of the functional relationship between the carrier density and the forward current is not required.

Two paths of carrier losses recombining outside the active layers are considered: (i) defect-related leakage current I_{defect} via surface, hetero-interface, or other defective areas and (ii) overflow leakage current I_{overflow} surpassing the active layers. These leakage currents result in the IE not being ideal. As the forward voltage increases, the defect-related leakage current I_{defect} appears at low bias voltages and saturates at a finite density of trapping centres. After then, most of the carriers begin to inject into the active layers and recombine there with the IE increasing. As the bias voltage increases further, I_{overflow} starts to flow at a certain bias and becomes a dominant leakage-current component over I_{defect}, which in turn decreases the IE again. In this picture, there should be a certain current, called the reference current I_{ref}, at which the IE is maximized.

The idea to find I_{ref} is as follows: As the current I increases, a_1 and a_2 generally vary very slowly compared to X and Y. Thus, the functions a_1 and a_2 are obtained by solving two simultaneous equations from Equation (96) with two nearest experimental data $(X_{\mathrm{i}},\ Y_{\mathrm{i}})$ and $(X_{\mathrm{i+1}},\ Y_{\mathrm{i+1}})$. In Equation (98), the a_2 coefficient is inversely proportional only to the IE. Thus, I_{ref} is selected as a current at which a_2 is the minimum. Once a set of a_1 and a_2 is found as a function of *I* or *X*, then the RE at a current *I* is calculated by Equation (99).

As a first step, $\eta_{\mathrm{IE}} = 100$ % is assumed at $I = I_{\mathrm{ref}}$ since I_{defect} saturates at a much smaller current than I_{ref}, i.e., $I_{\mathrm{defect}} \ll I_{\mathrm{ref}}$, and I_{overflow} is not so large yet. $\eta_{\mathrm{RE}}(I_{\mathrm{ref}})$ is then found for the set of $(X_{\mathrm{ref}}, a_{1,\mathrm{ref}}, a_{2,\mathrm{ref}})$ at I_{ref}, using $\eta_{\mathrm{RE}} = a_2 X^2 / (a_1 X + a_2 X^2)$. Subsequently, $\eta_{\mathrm{IQE}}(n_{\mathrm{ref}})$ at I_{ref}, i.e., $\eta_{\mathrm{IQE,ref}}$ is obtained by using already known values of $\eta_{\mathrm{IE}}(I_{\mathrm{ref}}) = 100$ % and $\eta_{\mathrm{RE}}(n_{\mathrm{ref}})$ from $\eta_{\mathrm{IQE,ref}} = \eta_{\mathrm{IE,ref}} \cdot \eta_{\mathrm{RE,ref}}$. Once $\eta_{\mathrm{IQE,ref}}$ is known, $\eta_{\mathrm{IQE}}(I)$ can be calculated at any current I from

$$\eta_{\mathrm{IQE}}(I) = \eta_{\mathrm{IQE}}(I_{\mathrm{ref}}) \frac{\eta_{\mathrm{EQE}}(I)}{\eta_{\mathrm{EQE}}(I_{\mathrm{ref}})}\,. \tag{100}$$

Note that the RTRM method does not presuppose any initial value on the IQE at the reference current: the IQE is purely calculated by using Equation (99) and the assumption IE = 1.

7.5 Example of the RTRM

Figure 19 shows a flow chart of calculation procedure of the IQE based on the proposed AB model at a fixed temperature of room temperature. For demonstration of the method, a commercial lateral-type InGaN/GaN MQW blue LED is utilized, which was grown on a c-plane

sapphire substrate. The chip size of the device is 740 μm × 600 μm. Its peak emission wavelength is approximately 450 nm at room temperature. The LED was driven by a Keithley semiconductor parameter analyser and the light output power was collected by a Si photodiode under the pulsed current driving condition (pulse period: 100 μs, duty cycle: 1 %) for minimum self-heating effect. Experimental curves obtained at each step of Figure 19 are shown in Figure 20.

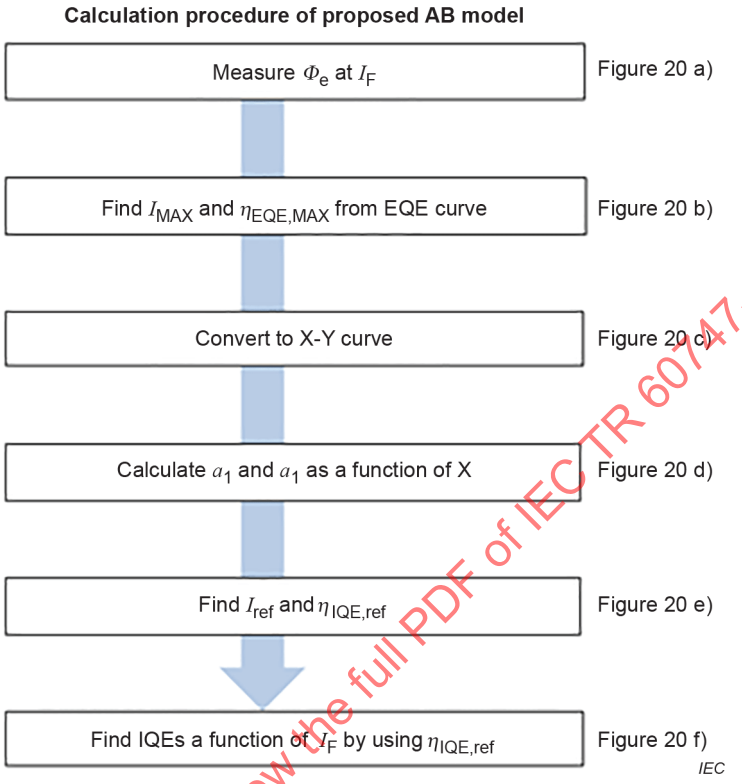

Figure 19 – IQE calculation procedure as a function of current based on the RTRM

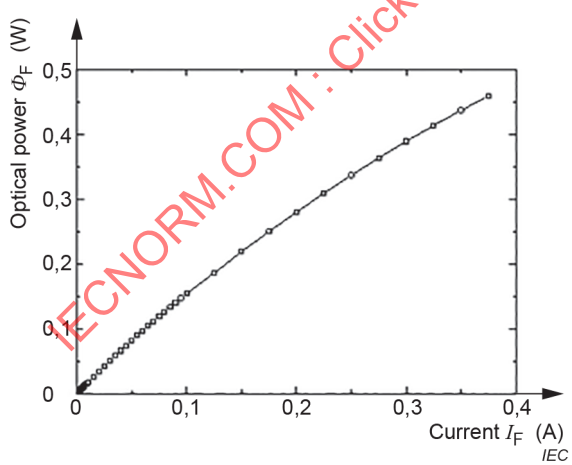

a) radiant power versus current,

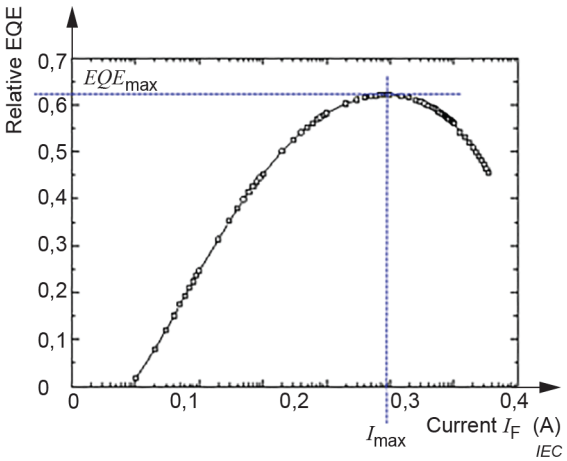

b) relative EQE versus current

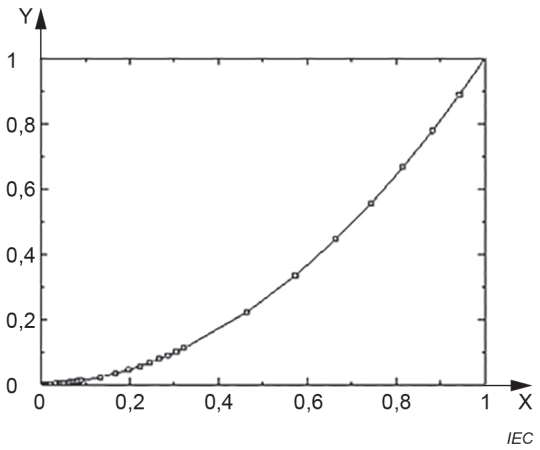

c) Y versus X converted from Figure 20 a)

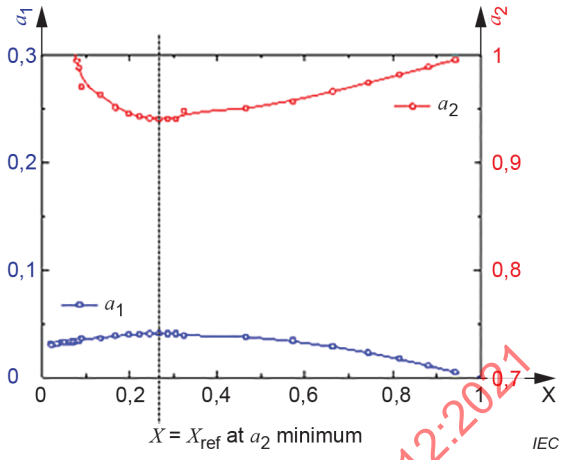

d) a_1 and a_2 versus X in order to find the reference point

$$\eta_{IQE,ref} = \frac{a_{2,ref} X^2_{ref}}{a_{1,ref} X_{ref} + a_{2,ref} X^2_{ref}}$$

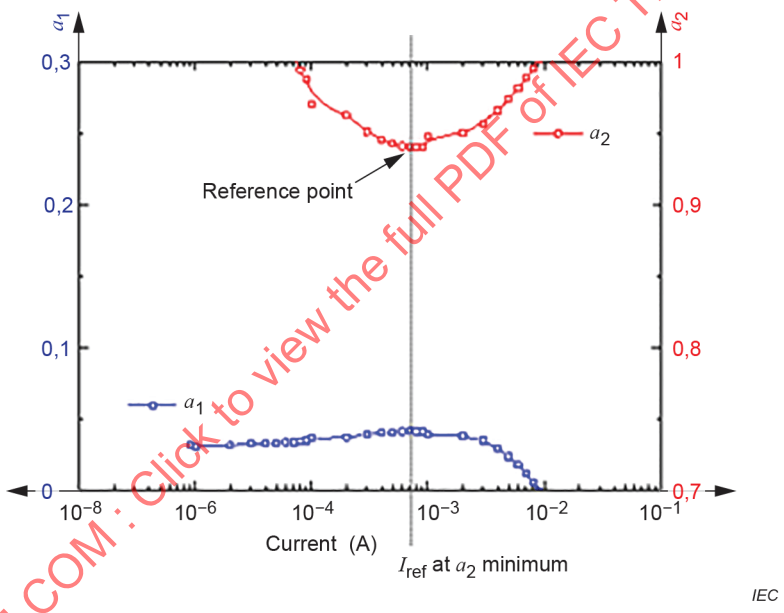

e) the IQE at the reference point

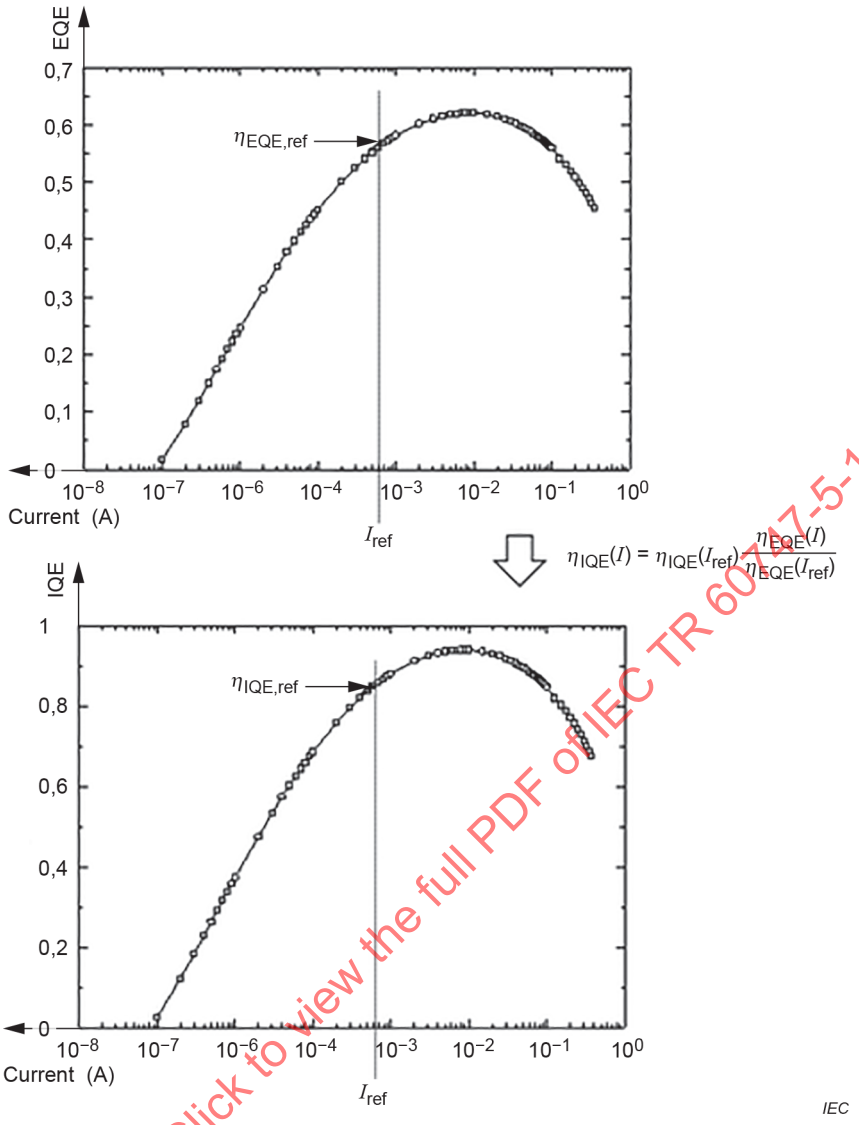

f) the IQE versus current

Figure 20 – Example of the IQE calculation based on the RTRM

7.6 Comparison of IQEs by the TDEL and the RTRM

For ensuring the reliability and accuracy of the RTRM, both the TDEL and the RTRM were applied and compared experimentally. In the TDEL experiment, the LED was cooled down from 300 K to 50 K in a helium closed-cycle cryostat.

$\eta_{IQE}(I)$ by the RTRM is compared with the ones from the TDEL method for the blue LED as shown in Figure 21 a) and b), respectively. In the TDEL measurement [Figure 21 a)], the maximum η_{EQE} at the cryogenic temperatures (100 K and 50 K in this case) represents $\eta_{IQE,ref} = 100\ \%$ and $\eta_{IQE}(T,I)$ at any temperature T is calculated from $\eta_{IQE}(T,I_{ref}) = \eta_{EQE}(T,I)/\eta_{EQE,ref}$. In Figure 21 b), the reference I_{ref} at each temperature T is calculated by the RTRM assuming that $\eta_{IE}(T,I_{ref}) = 1$ and $\eta_{RE}(T,I_{ref}) = \eta_{IQE,ref}(T)$. $\eta_{IQE}(T,I)$ is calculated from Equation (100). The peak values of $\eta_{IQE}(I_p)$ at 300 K estimated by the TDEL and the RTRM are 82 % and 80 %, respectively. It is thought that the measurement results by both methods are quite consistent, considering the assumptions behind the two methods.

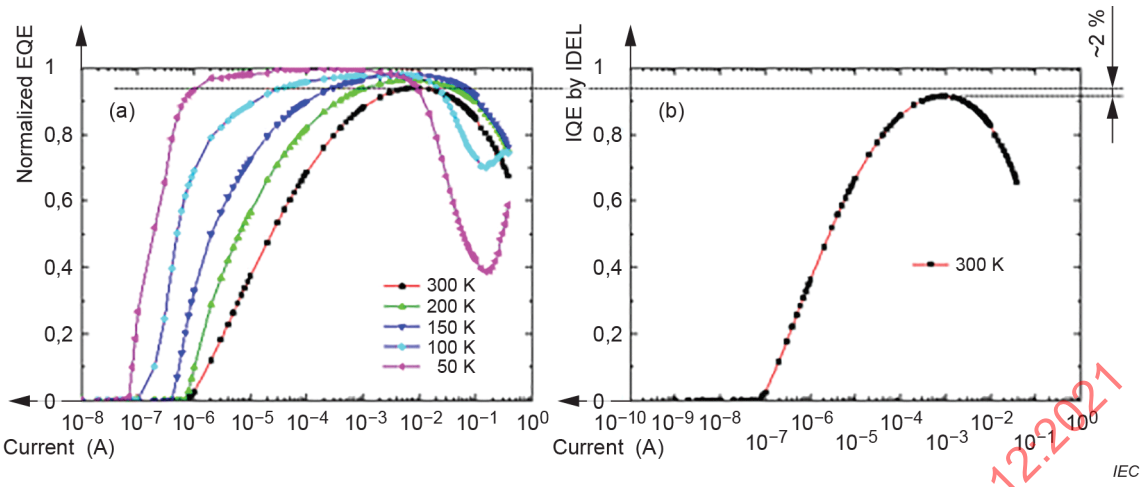

Figure 21 – Comparison of the IQEs evaluated by (a) the TDEL and (b) the RTRM

7.7 Summary of the RTRM

In summary, a simple and unique IQE measurement method at any operating temperature T has been presented and demonstrated. The RTRM is theoretically based on the semiconductor rate equation with A and B recombination coefficients depending on the carrier density and utilizes only experimentally measurable quantities of radiant power, current, and voltage. The measurement procedure of the RTRM is quite similar to the TDEL method where η_{IQE} at the maximum η_{EQE} is considered as 100 % and the ratio of EQEs is linearly proportional to η_{IQE}. The RTRM also finds the reference current I_{ref} at which $\eta_{IQE,ref}$ is exactly known. Then, η_{IQE} at an arbitrary current I can be obtained from the relative ratio of $\eta_{EQE}(I)/\eta_{EQE}(I_{ref})$. Unlike the TDEL, however, the reference current I_{ref} is found at which η_{IE} is considered as 100 % but η_{RE} is less than 100 %. With η_{IE} of 100 % at I_{ref}, η_{RE} at I_{ref} as $\eta_{IQE,ref}$ can be calculated by using infinitesimal changes of η_{IQE}. Once $\eta_{IQE}(I_{ref})$ is found as $\eta_{IQE,ref}$, $\eta_{IQE}(I)$ at any current I is easily calculated from the experimentally measured $\eta_{EQE}(I)$. The proposed method of measuring $\eta_{IQE}(I)$ has been applied to the InGaN-based blue LED and compared with the results by the TDEL.

8 The RTRM versus the TDEL and the constant ABC model: comparisons

Three IQE measurement methods of the TDEL, the constant ABC model, and the RTRM are applied to a same blue LED chip and the results are compared. A commercial lateral-type InGaN/GaN MQW blue LED grown on a c-plane sapphire substrate with a chip size of 1 100 × 650 μm^2 has been selected.

The LED was driven under the pulsed-current driving condition (pulse period: 1 ms, duty cycle: 1 %) for minimum self-heating effect. The LED sample was cooled down from 300 K to 20 K in a helium closed-cycle cryostat.

Radiant powers from the sample measured at various temperatures are shown in Figure 22. The maximum radiant power at 250 mA is obtained at a medium temperature of 200 K, not at the lowest cryogenic temperature of 20 K, which is due to the efficiency droops acting differently with current and temperature. Shown in Figure 23 a) are emission spectra on a linear scale at a current of 250 mA for various temperatures. As temperature decreases from 300 K to 200 K, 100 K, and 20 K, the peak wavelength shows the U-like shift from 448 nm to 445 nm, 444 nm, and 445 nm, respectively. It is believed that this U-like shift of the peak wavelength is due to a trade-off between the bandgap widening and the thermal heating by increasing resistance. It is also seen that a subpeak around 460 nm becomes more pronounced. Actually, there are a

series of subpeaks when the emission spectra are plotted on a log scale [Figure 23 b)]. The more pronounced subpeaks with decreasing temperature have been reported as the longitudinal-optical (LO) phonon replicas of the main peak [56], [57]. On the other hand, an LED chip has finite reflectivities at the interfaces between metallic surfaces, epitaxial layers, and substrate surfaces. Since the optical losses are reduced with decreasing temperature, the Fabry-Perot effect is another possibility of the subpeaks. More investigation may be necessary to further identify the exact cause of the subpeaks.

The I-V characteristics measured at various temperatures are depicted in Figure 24. It is seen in the reverse-bias region that the generation currents via defects at reverse biases less than −5 V are negligible at all temperatures and becomes smaller with decreasing temperature. On the other hand, it is not easy in the forward-bias region to identify the amount of leakage currents that do not recombine in the active layers. Here, the RTRM is used to find the leakage current at relatively low current levels.

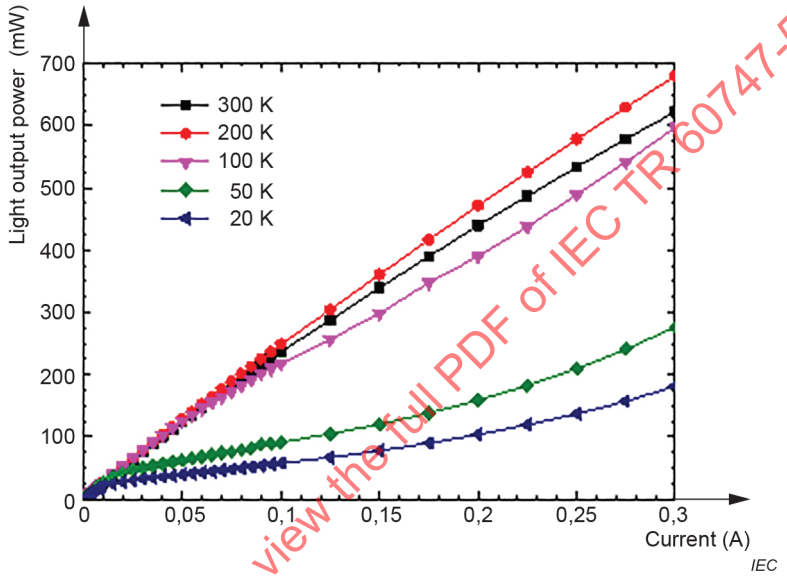

Figure 22 – Radiant power versus current of a blue LED sample measured at various temperatures

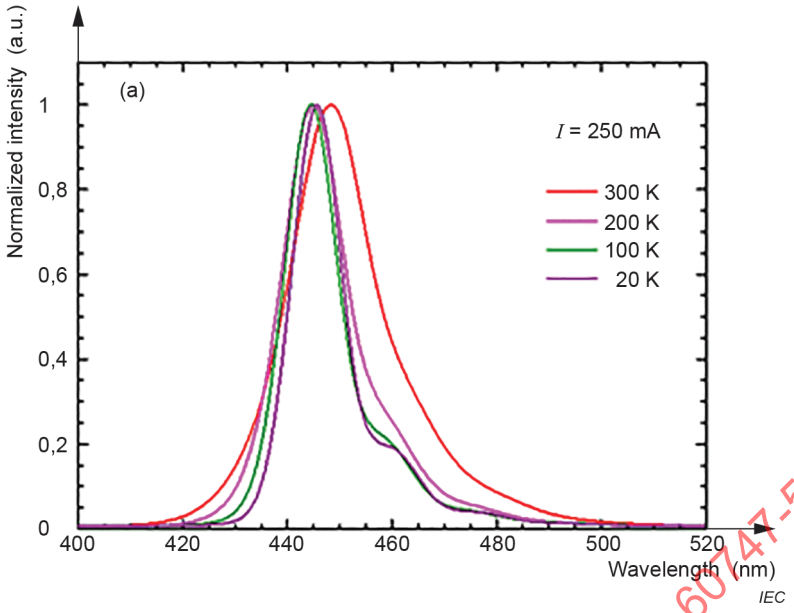

a) Linear scales measured at various temperatures

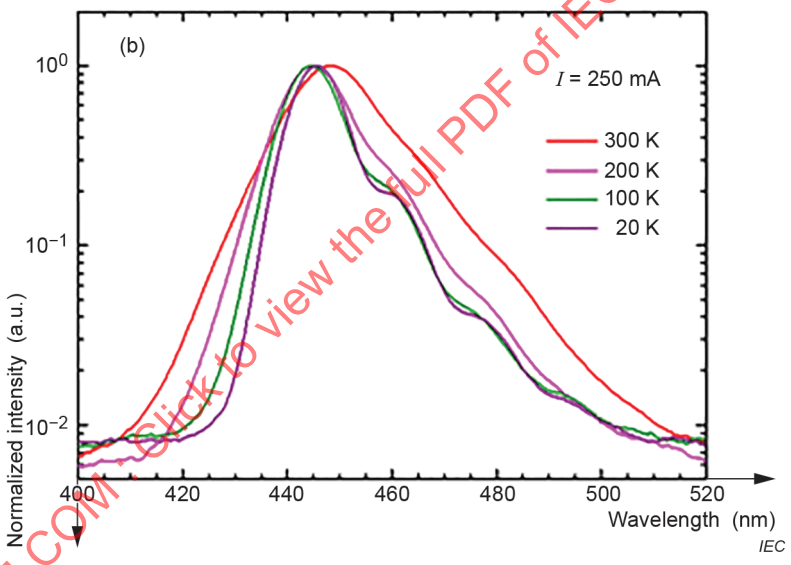

b) Log scales measured at various temperatures

Figure 23 – Normalized intensities on linear and log scales measured at various temperatures

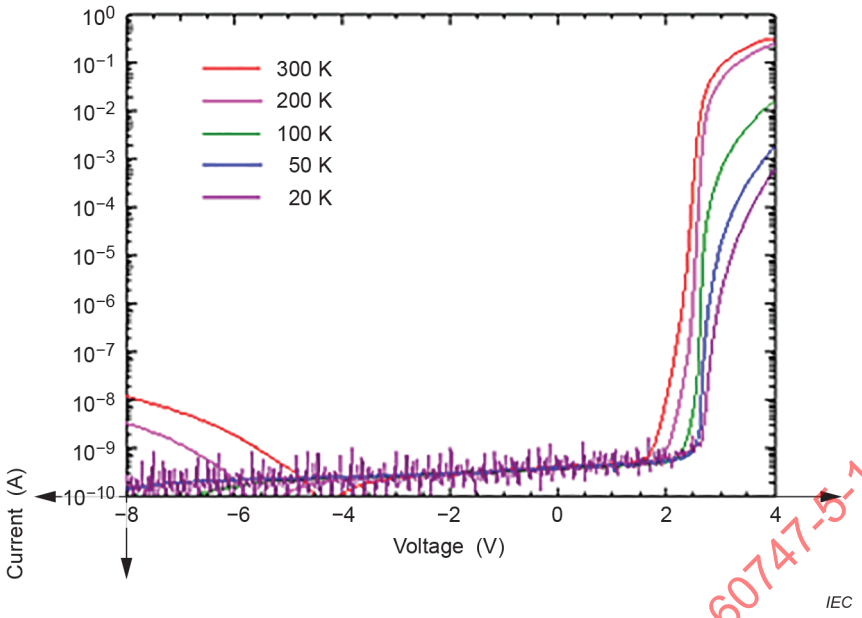

Figure 24 – *I-V* characteristics at various temperatures

Figure 25 depicts a_2 obtained by solving two simultaneous equations for two nearest experimental data from the converted X-Y graph according to Equations (96), (97), and (98). For this sample, the obtained a_2's are not constant, implying that $\eta_{IE} \neq 1$ over the current ranges investigated. At 300 K, a_2 decreases for currents beyond ~10^{-5} A, approaches a minimum at 2 x 10^{-3} A (= I_{ref}), and then increases. This indicates that the IE, inversely proportional to a_2, approaches a maximum, which is considered as 100 %, and then decreases. For very small currents below ~10^{-5} A denoted as region I, the rapid change in a_2 could be due to the leakage current I_{defect} before the onset of the radiative current flowing into the active layers. It should be noted that such a leakage current is different in each device and operating condition that the influence of the leakage on the IQE calculation should be carefully considered in every IQE measurement. For a current range of 10^{-5} to 2x10^{-3} A, denoted as region II, a_2 decreases and the IE increases. This is due to the saturated I_{defect} and the monotonic increase of the radiative current. For $I > I_{ref}$, denoted as region III, the carrier overflow from the InGaN QWs to the p-GaN clad layer should be responsible for the increasing a_2 and decreasing η_{IE}. As temperature is decreased, it is seen that a_2 becomes flattened near the minimum, indicating that η_{IE} does not vary as much as at room temperature. This is reasonable because η_{IE} is not expected to change much at cryogenic temperatures with vanishing leakage paths owing to the defect freeze-out. This trend is confirmed later with the TDEL measurements (Figure 26).

Figure 26 shows the measured IQEs as a function of current by applying the TDEL (solid lines) and the RTRM (symbols). The IQEs at the reference currents from Equation (99) are estimated to be 0,876, 0,959, and 0,978 for 300, 150, and 20 K, respectively, and other IQE values are calculated by using Equation (100). The maximum EQE at the cryogenic temperature is selected as IQE of 100 % (I_{ref} = 2 × 10^{-5} A, T_{ref} = 20 K in this case) and $\eta_{IQE}(I, T)$ at any temperature T is calculated from Equation (90). In the TDEL, one should pay attention to experimentally confirming the saturation characteristics of the maximum η_{EQE} at the reference point by changing both temperature and current. As shown in Figure 26 by solid lines, $\eta_{IQE} > 99$ % are measured at certain current ranges [(7 × 10^{-6}) − (2 × 10^{-4}) A for 20 K and (2 × 10^{-5}) − (5 × 10^{-4}) A for 50 K).

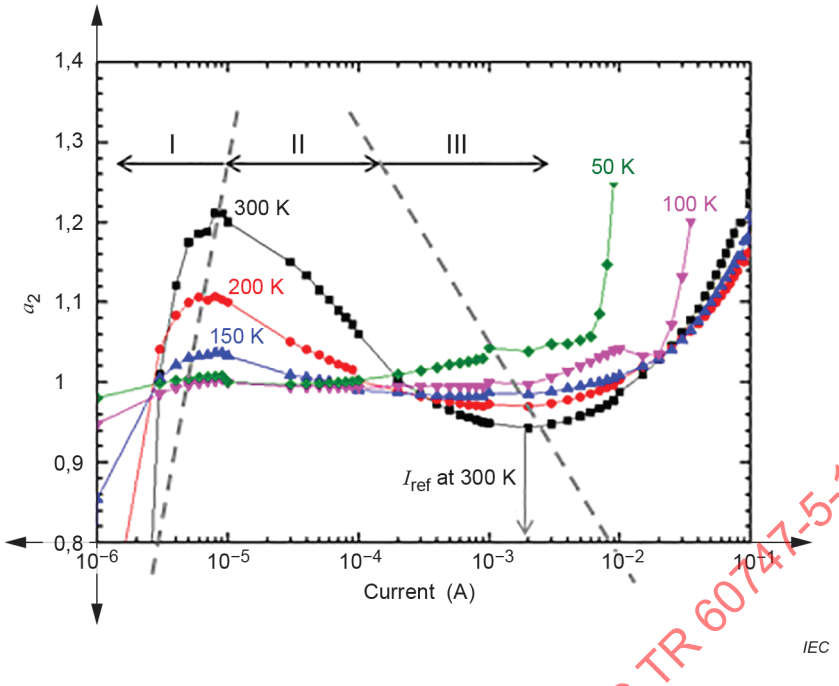

Figure 25 – Calculated a_2 as a function of current for various temperatures. I_{ref} at 300 K is the current giving the minimum value of a_2 in region II.

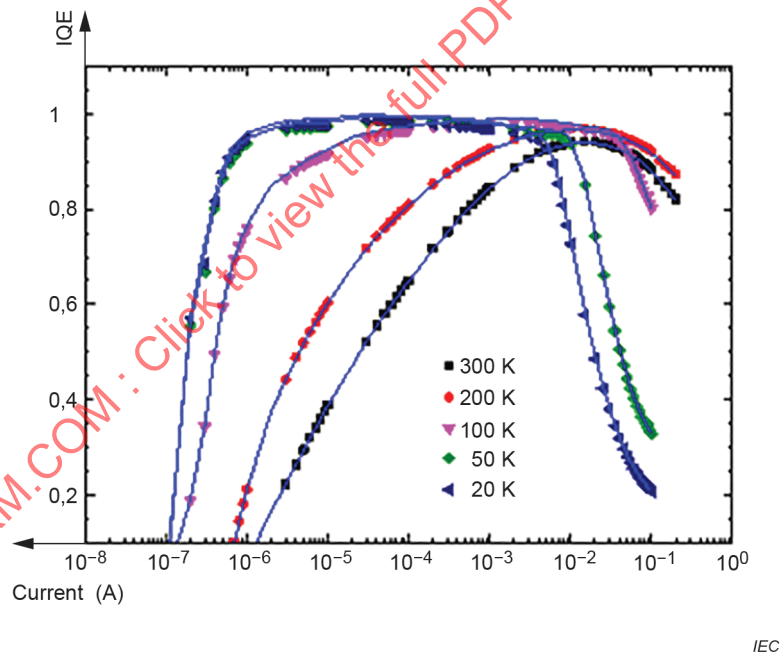

Figure 26 – IQEs obtained by the RTRM (symbols) and the TDEL (solid lines) at various temperatures

The calculation procedures of the two methods, the RTRM and the TDEL, are very similar once η_{IQE} at a reference point is found. η_{IQE} values at other currents are then calculated from η_{IQE} at the reference point by taking the relative ratios from the experimental η_{EQE} values. Thus, the shapes of the IQE curves at a certain temperature by the two methods are identical to each other except the peak IQE values. The maximum η_{IQE} values by the TDEL and RTRM at 300 K are almost the same as 0,941 and 0,943, respectively. The maximum IQE values by the two different methods agree very well within 2 % for all temperatures. The small discrepancy in the maximum η_{IQE} obtained by the two methods could occur from the measurement inaccuracies

in radiant power as well as the temperature dependency of the LEE [27]. The LEE can vary with temperature especially when the energy of the spontaneous emission from the active layer of an LED is close to the bandgap energy or absorption edge of the surrounding materials. Variations in LEE with InGaN-based LEDs have been reported to be as much as 4 % to 6 % over temperatures from approximately 10 K to 300 K [27],[58],[59].

Finally, the error involved in the RTRM by assuming $\eta_{IE} = 1$ at I_{ref} is discussed. Using the data obtained at 300 K, the left axis of Figure 27 shows $a_2(I_{ref})/a_2(I)$, which represents the IE. On the right axis, the theoretical IE, that is, $(I - I_{leak})/I$, is given for a *constant* leakage current I_{leak}. Naturally, the theoretical IE quickly approaches unity as the total current increases. From the various ratio of I_{leak} to I_{ref}, it is seen that the IE from a_2 roughly follows the functional shape of the theoretical IE between the leakage of 0,4 % and 0,6 % of I_{ref}. This indicates that at I_{ref} the IE is considered to be 99,4 % in the worst case. From this exercise, it is considered that the assumption $\eta_{IE} = 1$ is reasonable, with only a minimal error included. On the other hand, samples with very high leakage currents should be treated carefully as they may not satisfy the assumption $\eta_{IE} = 1$ at I_{ref}.

In fact, theoretical background of the constant AB model is quite similar to that of the RTRM except that the former utilizes a wide range of relatively low current levels with $\eta_{IE} = 1$ and the latter selects one reference current with $\eta_{IE} = 1$. Thus, the key is to find the current at which assuming the IE of 100 % is valid. In this sense, a lot of information can be obtained from the calculation of a_2 as a function of current as demonstrated in Figure 27.

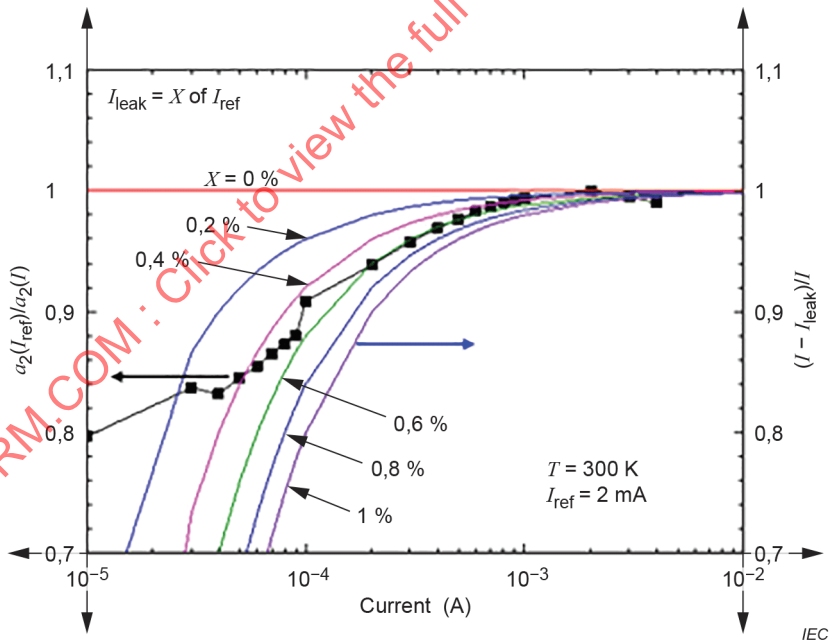

Figure 27 – Comparison of the IE obtained from a_2 at 300 K (left axis) and the theoretical IE for constant I_{leak} (right axis)

The experimental data measured at 300 K is also fitted by using the constant ABC model [Equation (81)]. The sample under test has $I_{max} = 15$ mA so that the normalized EQE curve is theoretically calculated with η_{max} as a fitting parameter. Figure 28 shows the calculation results in comparison with the experimental data. It is seen that $\eta_{max} = 90$ % gives the best fit for the data near I_{max}. Still, deviations from the experimental data are observed for lower and higher currents than I_{max}.

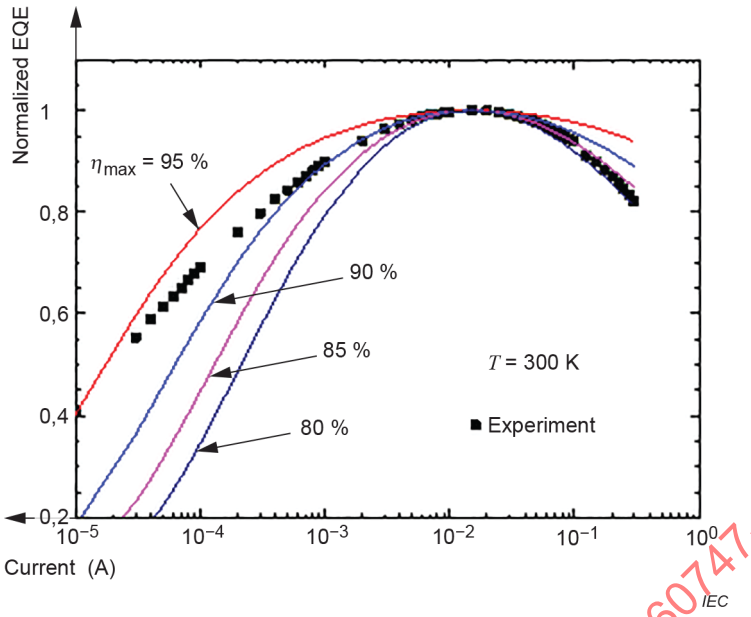

Figure 28 – Normalized EQE and the fitting by the constant ABC model

With $\eta_{max} = 90$ %, the relative ratios of the SRH, radiative, and Auger recombination currents to the total current can be plotted as shown in Figure 29. At $I_{ref} = 2$ mA of the RTRM, denoted by the dotted line, it is seen that the Auger recombination current in the constant ABC model is 1,6 % of the total current. With this level of contribution by the Auger recombination, it is considered that the Auger recombination term can be neglected when finding the reference point in the RTRM. In fact, the Auger recombination current in the constant ABC model can correspond to the current leakage via carrier overflow in the RTRM for certain constants A and B. In this picture, this negligible Auger recombination current at I_{ref} can be considered as another vindication that the carrier leakage can be neglected at the reference point in the RTRM.

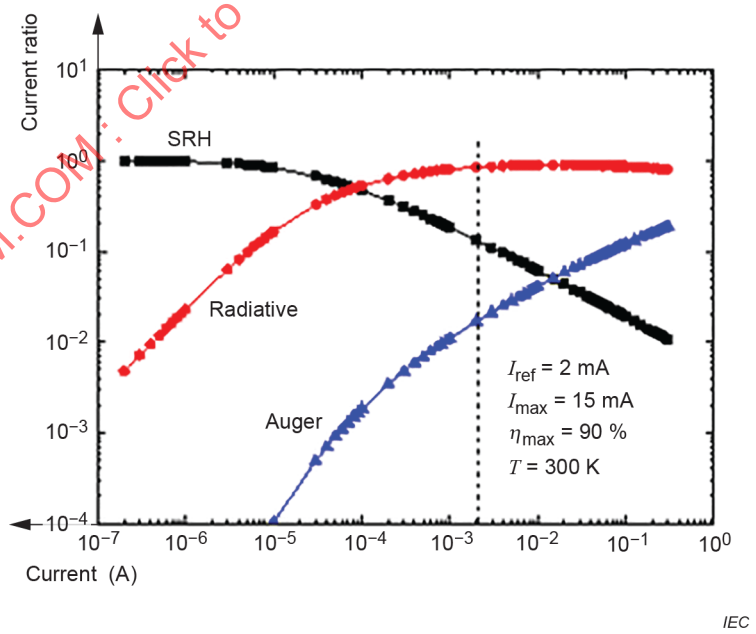

Figure 29 – Ratio of the SRH, radiative, Auger recombination currents to the total current

Three IQE measurement methods of the RTRM, the TDEL, and the constant ABC model have been compared. All three methods utilize the experimentally measured EQE curve. In the TDEL,

$\eta_{IE} = \eta_{RE} = 1$. The IQE at room temperature is then calculated by the relative ratio of the EQE values at room temperature to the cryogenic reference point under the assumption of a constant LEE for all temperatures. In fact, the LEE of an LED may not be constant: it typically becomes smaller at higher temperature. Moreover, its temperature dependence becomes larger as the emission wavelength of an LED becomes longer from visible to infrared spectral ranges, which results from the increase of optical losses in epitaxial layers whose bandgap energies are not so much different from that of the active layer. Therefore, the TDEL can be recommended to be used for InGaN-based visible LEDs rather than longer-wavelength GaAs- or InP-based LEDs. On the other hand, the RTRM and the constant AB(C)-models under a given temperature assume only the constant LEE with current, which is more reasonable than the TDEL.

The conventional constant AB(C)-models roughly assume the IE of 100 % for certain current ranges near the onset of light emission or the EQE peak. In real LEDs, however, it is hardly true that the IE is ideal since the leakage current via defects near the onset of light emission and the carrier overflow near the EQE peak are frequently observed. The RTRM avoids such technical concerns in the conventional AB(C)-models. In this consideration, it is thought that the RTRM is the most accurate and reliable of the methods considered herein.

9 LED performance issues related to the IQE measurement

9.1 Various LED efficiency measurement

The PE can be obtained in a straight-forward way by using Equation (1). Measuring methods of the radiant power Φ_e and the electrical V_F and I_F are already defined in IEC FDIS 60747-5-6:2016 (see Table 1). In order to define the EQE, one needs to find the average photon energy $h\bar{\nu}$, using Equation (3). Once the average photon energy is defined, the EQE can be obtained by the definition given by Equation (4). Using the obtained PE and EQE, the VE can now be calculated by using Equation (5) as $\eta_{VE} = \eta_{PE} / \eta_{EQE}$.

To separate the efficiencies further, the IQE is required. Methods of obtaining the IQE are discussed in detail in sections 6 and 7. Once the IQE is determined by a certain method like the RTRM, the LEE can now be obtained by using Equation (8): $\eta_{LEE} = \eta_{EQE} / \eta_{IQE}$.

Here, it is demonstrated how one can measure various LED efficiencies constituting the PE. As individual efficiencies represent different physical processes, separating various efficiencies is very beneficial in remedying any problems and enhancing the performance of LED chips further. For this purpose, a commercial lateral-type InGaN/GaN MQW blue LED grown on a c-plane sapphire substrate with a chip size of (740 × 600) μm^2 is utilized. The peak wavelength is approximately 450 nm at 293 K. The LED is driven under the pulsed-current driving condition (pulse period: 1 ms, duty cycle: 1 %). The pulsed-current driving is for avoiding the self-heating and is not essential for the IQE measurement by the RTRM: measurement of the radiant power by the CW current injection is also OK even though the chip is heated at high currents. The IQE measured under CW current injection may reflect the IQE in real operating conditions. If one wants to measure the intrinsic LED characteristics at a given chip temperature, however, the pulsed-current driving is recommended. The response of an LED operated under this pulsed-current injection is still considered as steady state since the pulse is relatively long (in the order of 1 ms).

In the following example, the absolute radiant power, not the relative radiant power, is measured since the PE, EQE, and LEE measurements require the absolute radiant power. If one wants to measure the IQE only, the measurement of the relative radiant power is sufficient.

Figure 1 in 4.3 has shown the sequence of measuring various LED efficiencies separately and quantitatively. Each step in Figure 1 can be followed to demonstrate the measurement of each efficiency.

First, the PE should be obtained from the radiant power (voltage) versus current measurement (Figure 30). Once the radiant power and forward voltage are obtained as a function of currents, the PE can be evaluated by taking the ratio of the radiant power to the input electrical power, as depicted by line 1 in Figure 32.

Second, the emission spectra is measured and the mean photon energy is calculated as given by Equation (3). Figure 31 a) and b) show the emission spectra at various forward currents and the mean photon energy thus obtained. Using definitions given in Table 1, the EQE is calculated by taking the ratio of the number of photons emitted to free space per second to the number of electrons injected into the LED per second. The result is shown as line 2 in Figure 32.

Third, the VE is then calculated by taking the ratio of the PE to the EQE, whose result is shown as line 3 in Figure 32. Note that at currents below approximately 20 mA, the VE exceeds 100 %, indicating that the mean photon energy is actually larger than the mean electrical energy supplied by the power supply, the fact only possible when one includes thermal energy into account. At low voltages below the mean photon energy divided by the elementary charge, the carriers are still injected into the active region with the help of thermal energy in the lattice. This interesting phenomenon has been reported elsewhere by various names such as electroluminescent refrigeration, opto-thermistic cooling, or thermo-photonic cooling as the cooling of the lattice occurs when the carriers take away the thermal energy from the lattice and get injected into the junction [136]-[138].

Fourth, now one needs to measure the IQE accurately. Using the RTRM, the IQE is obtained as shown by line 4 in Figure 32.

Lastly, once the IQE is obtained, the LEE can be obtained by taking the ratio of the EQE to the IQE. The LEE thus obtained is approximately 66 % (line 5 in Figure 32).

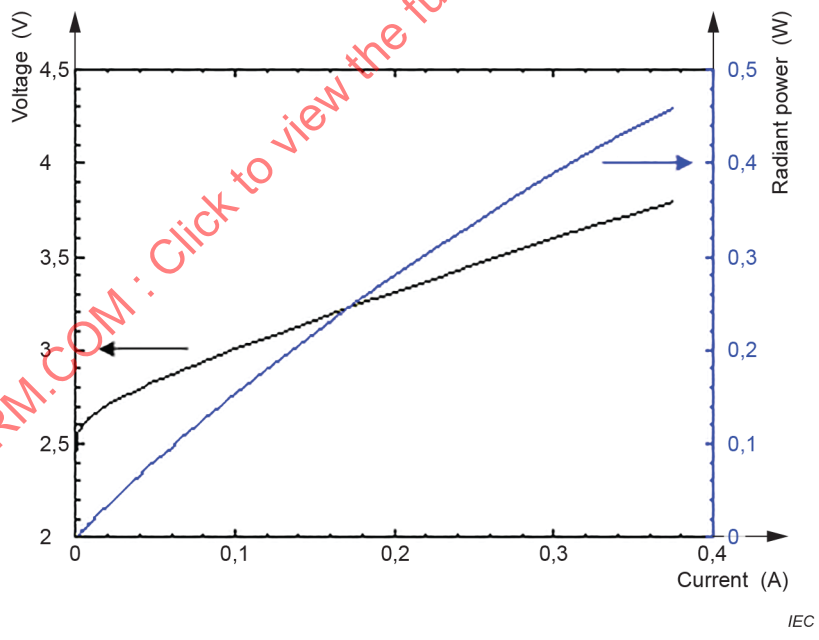

Figure 30 – Radiant power and forward voltage as a function of forward current

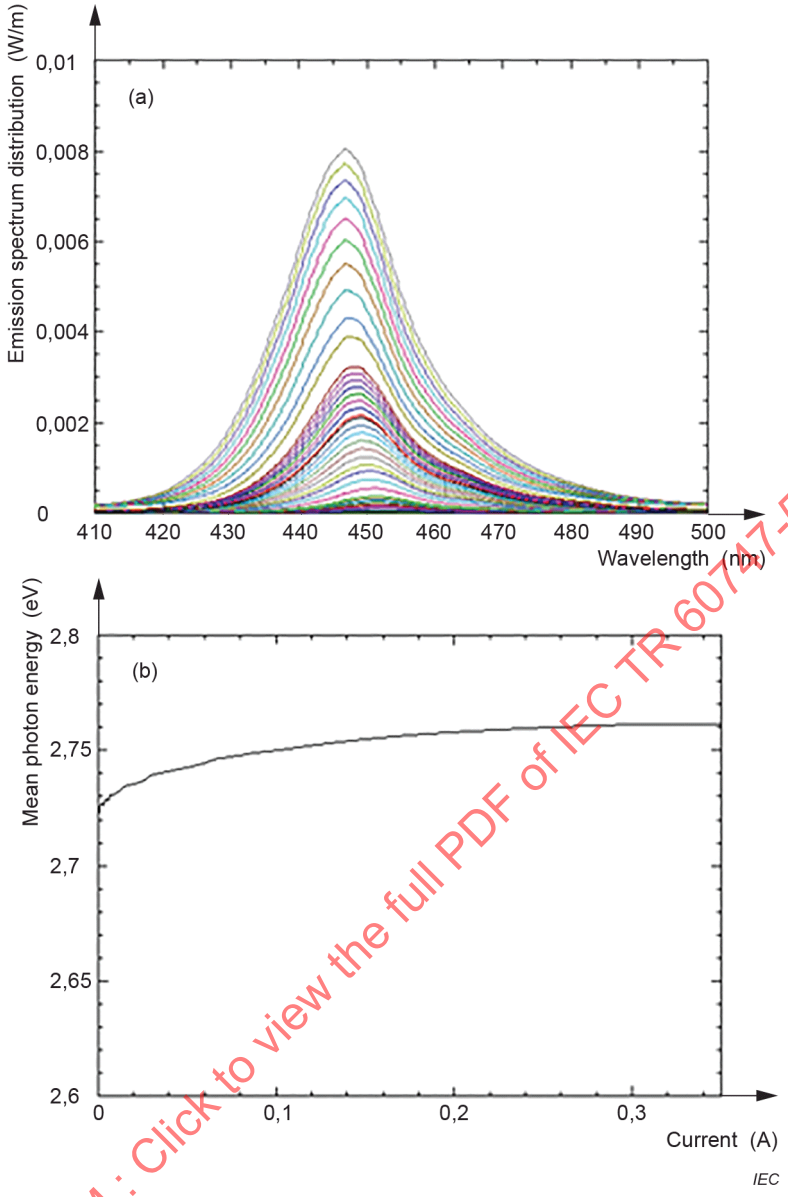

Figure 31 – Calculation of the mean photon energy from the emission spectra

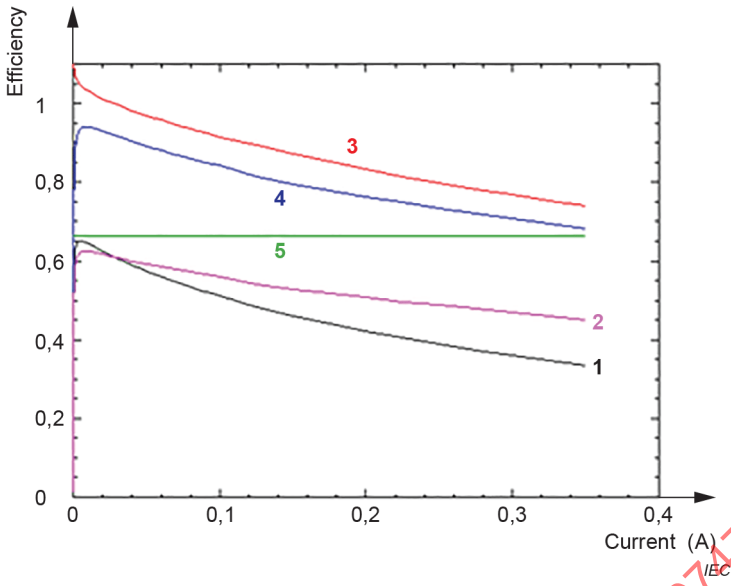

Key

1: PE;

2: EQE;

3: VE;

4: IQE;

5: LEE.

Figure 32 – LED efficiencies as a function of forward current

9.2 Radiative and nonradiative currents

The curve of total forward current versus applied voltage (I-V) of a pn junction diode is typically modelled by the Shockley equation. The Shockley equation was originally developed for a *pn* homojunction diode based on Si or Ge, where most of the carriers under forward bias are transported and diffused to the pn junction and recombine there by either the band-to-band or the SRH recombination processes. Note that both processes are nonradiative in indirect-bandgap Si or Ge semiconductors. Such carrier transport and recombination processes in the Shockley equation are represented by the diode ideality factor, the reverse saturation current, and the junction potential drop. However, in LEDs made of III-V heterojunction semiconductors, there exist a number of carrier transport and recombination processes much different from those in Si homojunction pn diodes. Contrary to the Si pn diode, the total forward current in the LED can be divided into two distinct current components representing different carrier recombination processes, namely, the radiative recombination current, I_{rad}, and the nonradiative recombination current, I_{nonrad}. In this sense, the conventional Shockley equation is not adequate to describe the I-V characteristics of the LED accurately. While there have been frequent investigations of total forward current I vs. applied voltage V by the Shockley equation, the data of I_{rad} and I_{nonrad} versus V still requires a deeper analysis for the LED devices.

Here, it is attempted to understand the physical interrelationships of current, voltage, radiant power, and eventually, the PE of the InGaN-based blue LEDs at high injection currents. The separation of the total forward current into the radiative current, I_{rad} and nonradiative current, I_{nonrad} is achieved by utilizing the experimental IQE curve. Then, each current is carefully investigated as a function of applied voltage. This approach can enable to conclude later that the IQE and the operating voltage at high forward currents are physically related with the phase-space filling by the accumulated carriers in the active MQW region.

The total forward current I_F supplied to an LED can be decomposed into radiative and nonradiative currents:

$$I_F = I_{rad} + I_{nonrad} . \quad (101)$$

Using the radiative and nonradiative currents, the IQE can be re-expressed as follows:

$$\eta_{IQE} = \frac{I_{rad}}{I_F} = \frac{I_{rad}}{I_{rad} + I_{nonrad}} . \quad (102)$$

With the above relation, the radiative and nonradiative currents can be expressed:

$$I_{rad} = \eta_{IQE} I_F , \quad (103)$$

$$I_{nonrad} = I_F - I_{rad} = (1 - \eta_{IQE}) I_F . \quad (104)$$

Electrical power consumed by the radiative process (P_{rad}) in the LED can be expressed as

$$P_{rad} = I_{rad} V_F = \eta_{IQE} I_F V_F = \eta_{IQE} P , \quad (105)$$

where P is the total electrical power dissipated by the LED: $P = I_F V_F$.

Electrical power consumed by the nonradiative processes ($P_{non\text{-}rad}$) in the LED can be expressed as

$$P_{nonrad} = I_{nonrad} V_F = (1 - \eta_{IQE}) I_F V_F = (1 - \eta_{IQE}) P . \quad (106)$$

The power efficiency (η_{PE}) represents how much electrical power dissipated by the LED is converted to the radiant power (Φ_e):

$$\Phi_e = \eta_{PE} P . \quad (107)$$

Since $P = P_{rad} / \eta_{IQE}$ and $\eta_{PE} = \eta_{VE} \cdot \eta_{LEE} \cdot \eta_{IQE}$,

$$\Phi_e = \frac{\eta_{PE}}{\eta_{IQE}} P_{rad} = \frac{\eta_{VE} \cdot \eta_{LEE} \cdot \eta_{IQE}}{\eta_{IQE}} P_{rad} = \eta_{VE} \cdot \eta_{LEE} \cdot P_{rad} . \quad (108)$$

Figure 33 shows the measurement sequence of radiative and nonradiative currents when a specified forward current is applied.